Reply to anonymous referee 1

The authors would like to thank the referee for their review of the paper "Optical properties of laboratory grown sea ice doped with light absorbing impurities (black carbon)."

Changes made to the paper based on the comments are detailed below on a point-by-point basis:

The abstract feels rushed and confused compared to the rest of the paper and does not do the paper justice.
The abstract has been rewritten.

"*Radiative-transfer calculations of the light reflectivity and extinction coefficient in laboratory generated sea ice doped with and without black carbon demonstrate that the radiative transfer model TUV-snow can be used to predict the light reflectance and extinction coefficient of sea ice typical of first year sea ice containing typical amounts of black carbon and other light absorbing impurities. The experiments give confidence in the application of the model to predict albedo of other sea ice fabrics.*

Sea ices, ~30~cm thick, were generated in the Royal Holloway Sea Ice Simulator (~2000 L tanks) with scattering cross-sections measured between 0.012 and 0.032 m^2 kg^{-1} for four ices. Sea ices were generated with and without ~5 cm upper layers containing particulate black carbon. Nadir reflectances between 0.60 and 0.78 where measured along with extinction coefficients of 0.1 to 0.03 cm^{-1} (e-folding depths of 10-30 cm) at a wavelength of 500 nm. Values were measured between light wavelengths of 350 and 650 nm. The sea ices generated in the Royal Holloway Sea Ice Simulator were found to be representative of natural sea ices.

Particulate black carbon at mass ratios of ~75, ~150 and ~300 ng g^{-1} in a 5 cm ice layer lowers the albedo to 97%, 90%, and 79% of the reflectivity of an undoped ``clean'' sea (at a wavelength of 500 nm)."

Much of the modelling community will be put off / not find this paper due to the terminology used. I suggest also quoting e-folding depths as extinction coefficients as these are the terms currently used by the majority of sea-ice models.
Throughout the paper "extinction coefficients" are now referred to in addition to "*e*-folding depths" (for the "snow" community) and the following explanation has been added to the text:
"*At the completion of the experiment the extinction coefficient and e-folding depth are measured. The e-folding depth is the distance over which light intensity reduces to 1/e of its initial value and is the reciprocal of the extinction coefficient. The e-folding depth is reported in addition to the extinction coefficient.*"

The laboratory description feels short and underplayed, this is a new facility and it is very difficult to visualise with the current amount of information provided. I suggest significantly increasing the information provided about the facility, although some could go in the supplementary section. I feel this is important, especially if the authors plan on using this paper as a background reference point to further papers using the facility. Some of the broad comments here are brought up in more detail in the specific comments.
The laboratory description had now been expanded to include further details of the facility including a further annotated figure of the facility, and two figures demonstrating the capabilities of the sea ice simulator (temperature

profiles and daily reflectance measurements) and further technical specifications. These changes are described in more detail in the specific comments below.

Specific Comments: (Format for reference, e.g 5.4: refers to Page 5, line 4.)

1.3: Question the use of "simulated" throughout, it gives an initial impression of modelling rather than experimental. Could this be altered to laboratory or artificial or something similar?

The word "simulated" has now been replaced with "laboratory" throughout the manuscript.

Abstract General: It is not clear from the abstract what the focus of the paper truly is, and it feels rushed leaving more questions than useful data in its current form. I would suggest removing discussion of algae (as this is barely mentioned in the main manuscript) and refocussing the abstract on the less technical aspects. The mention of measuring e-folding and reflectance and then later calculating e-fold and reflectance from absorption and scattering values sounds confusing in an abstract and is confusing to the reader. I would remove technical detail in favour of adding extinction coeffcients which may be of more value to the readership.

The abstract has been completely rewritten. The discussion of algae has been removed from the abstract and the level of technical detail lowered.

3.9: I would argue that it is a medium sized facility, as somewhere like SERF is a large facility. Could this be phrased in a more impressive way? E.g. "sea-ice simulator designed to reproduce polar sea-ice growth conditions under UV and Visible lighting"

The phrase:

"*The sea ice simulator is a large scale, UK based, laboratory sea ice tank designed to replicate warmer polar temperatures, the ocean and UV and visible wavelengths of solar radiation.*"

Has been replaced with:

"*The sea ice simulator is designed to replicate a Polar sea ice growth environment under UV and visible wavelengths of solar radiation*"

3.14: What is the temperature stability of the cold room?

The following sentence has been added to the text:

"*The air temperature within the container varies by ± 1°C although thermocouples monitoring temperature at the ice surface show better temperature stability, whilst the temperature variation measured within the ice is less than the precision of the probes (± 0.2°C). Every 12 hours the chiller removes ice build-up on the cooling plant and the air temperature rises briefly by ~6°C.*"

4.Fig1. Is there wind shear across the tank? It'd be good to have it added to the Figure.

A 20" fan located above the sea ice directed 110 m^3 min^{-1} of room air onto the ice at an angle of ~45°. The air velocity across the surface of the ice was ~1.5 ms^{-1}. The velocity of the airflow produced by the fan has been added to figure 1.

The following text has also been added to the manuscript

"*An additional air fan, attached to the ceiling, blows cold, ambient air at the water surface, (~100 m^3 min^{-1}), increasing the heat flux from the ice surface, quickening ice formation and assisting the production of columnar ice (Weeks, 2010).*"

4.General. It'd be really nice to see the facility description fleshed out more, with some more technical details of what the chamber is capable of (especially as this is appears to be the first paper to come out from the laboratory). Some suggestions would be how temp / salinity of the ocean vary through time of an experiment as the ice grows, lighting consistency at the ice surface, room temperature vs time during ice growth. These are just suggestions, but it would be good to have more technical facility description. Could some annotated photos be added to go alongside the figures? This would not only allow a much better visualisation, but could well encourage potential collaborators.

Further technical details have now been added to the laboratory description, including:
- Annotated photos of the facility
- A further two figures (new figures 2 and 3) have been added to section 2.1 to demonstrate the facilities capabilities. Figure 2 shows the change in ice and water temperature profiles during ice growth. Figure 3 shows the change in ice reflectance during ice growth and the day-to-day reflectance stability of the optically thick ice.
- The following additional pieces of text have been added to section 4
  "*Figure 2 demonstrates that the temperature of the water beneath the sea ice is not thermally stratified, sea ice growth is from the surface downwards, ice temperature decreases linearly through the ice with depth and the ice surface temperature is at a constant -15°C*"
- "*The short term variability of the lamps was less than 0.1% (after an initial warm-up) on the timescale of the measurement of reflectivity or e-folding depth. Note that both the value of nadir reflectance (relative to a Spectralon panel) and light penetration depth are not dependent on the illumination irradiance providing the irradiance does not change during the measurement. Figure 3 shows the change in nadir ice reflectance during ice growth and the day-to-day reflectance stability of the optically thick ice.*"

5.14: Model # for the thermocouples? Details on precision / calibration if possible?

The following sentence has been added to this section: "*The precision on all the thermocouples at -15°C was measured as ± 0.2°C*"

6.7: Again, could an annotated photo be added for the set up or an extra figure? It may not be implicit for non-experimentalists to imagine.

An extra, annotated, photograph has been added to this section as part of figure 1.

7.7: Clarify, is the tank emptied at this point or is bleach added?

The sentences "*Between experimental runs the tank is periodically bleached to remove any algae that may have grown. No algae was visible to the naked eye*", has been changed for clarity to read "*The sea ice was melted and the resulting seawater was treated with aqueous hypochlorous acid (HOCl) and filtered between experimental runs to remove any algae that may have grown. No algae was visible to the naked eye*"

7.27. Can the authors clarify whether this is a range, or the result of two experiments? Is there any way of knowing where the differences in result occur from?

The value of 0.58 has been removed from the text and was an erroneous value left in from a previous edit.

8. Table 1: No mention of sigmascatt in the caption. Please add details.

The caption has been changed to include the sigmascatt, the caption now reads:

"Table 1: Optical and physical properties of sea ice for each run including the mass-ratio of black carbon added to the top layer of ice, density of ice and scattering cross-section (σ_{scatt}) of both the top and bottom layers of the ice. The uncertainty...."

9. Figure 2. Caption is not sufficient and needs fully re-composing.

The caption has now been changed to read "*Figure 2: a) Relative spectral absorbance of black carbon versus wavelength for various loadings of black carbon on the filter. b) Relative spectral absorbance versus wavelength for different mass loadings of polypropylene*"

11. Fig 3: It could be due to black and white printing, but the contrast seems very off. It is a really nice Figure to have, but it currently is not as clear as it could be.

Figure 3 (now figure 5) has been improved, previously it displayed well electronically as a pdf, but did not print well, so the image has been sharpened and annotated to make the black carbon particles clearer.

11.5: The authors should be commended here for using a secondary method to calculate an important parameter for the work. This sort of thing is often overlooked and should be done much more in many fields of science.

Thank you

14.3 Is there any way of further discussing the fabrics of the ice? Is there any information in the cores that could be used? Currently the images in the SI are too small to really ascertain anything structural but maybe there is information within those images, which could be enhanced to help interpret the variability?

It has not been possible to enhance the images of the ice fabric any further and the sample no longer exist as they were melted for density measurements.

15. Fig 7: Please add a scaled absorption of algae (and what type of algae) be added here.

An absorption cross-section for chlorophyll-A from Bricaud et al. (2004) from algal cells, and chlorophyll in ice from Mundy et al (2011) has been added to this figure to more clearly demonstrate the identity of the extra absorption.

17.16: (and 19.10:) How does the uncertainty in the e-fold fitting procedure propagate through? There is much discussion about the other parameters but I feel that this is overlooked and that there are sources of error which are not propagated from the experimental side? Is there an easy way to estimate this?

Section 5.1.4 "Uncertainty in derived scattering and absorption cross-section and black carbon mass ratio"

has been altered to read:-

"*Section 5.1.4 Uncertainty in derived scattering and absorption cross-section and black carbon mass ratio*

The determination of the cross-section for light scattering and absorption, described in section 4.2.2, depends on varying their values to reproduce the measured values of the e-folding depth and the nadir reflectivity within the experimental uncertainties of measured values of the e-folding depth and the nadir reflectivity, all as a function of wavelength. The latter assists in constraining the determination of the values of the cross-section for absorption and scattering. The propagated uncertainty in the determined values of the cross-sections for light scattering and absorption from uncertainties in either the value of the e-folding depth or nadir reflectivity in isolation have not been calculated as our method fits both e-folding

depth and reflectivity. Considering the experimental uncertainty in e-folding depth and nadir reflectivity gives a more representative uncertainty of the process. The uncertainty in the reflectance and e-folding depth measurement data of the undoped ice is shown in figures 7 and 8. Table 1 gives an indication of the uncertainty in the derived scattering cross-section which is estimated by varying the values of σ_{scatt} and σ_{abs} and still obtaining a good fit (by eye) to the experimental data within the uncertainties of the measured e-folding depth and nadir reflectivity.

20.25: Would the extra ice at the side have any impact on the e-folding depth?

The *e*-folding depth is measured more than three *e*-folding depths away from the sides of the tank so the extra ice would have no effect on measured *e*-folding depth values. We have added the following comment to the text "*All measurements of the e-folding depth were made more than three e-folding depths from the sides of the tank so that any extra ice growth at the edges of the tank would no impact on the measurements.*"

21.4: It is my feeling that if light is being reflected back from the base of the tank, then there would be excess light within the ice at depth, which would result in the e-folding depth becoming longer and not shorter. I would also disagree with the authors comparison to the blue ice seen in Grenfell and Maykut (1977) as this is described as "ice saturated, but not covered, with melt water". The ice created here is fresh, "dry" ice and has not been subjected to melt metamorphism and structural change such as the one described in Grenfell and Maykut 1977, and should not be compared as such.

The reference to the first year blue ice has been removed from the text, as has the explanation for the shorter e-folding depths being attributed to light reflected off the bottom of the tank. The paragraph now reads: "*Typical extinction coefficients of sea ice at around 500 nm are around 0.03 cm^{-1} (Grenfell,1977). Calculated extinction coefficients for the laboratory grown ice range from 0.1-0.03 cm^{-1}.*"

Technical Comments:

2.26 Unclear, are these the first experiments or just the first experiments using TUV-snow?

The sentence "*The study presented here are the first experiments with the Royal Holloway Sea Ice Simulator to evaluate the TUV snow model for undoped sea ice….*" has been changed for clarity to read "*The study presented here includes the first experiments with the Royal Holloway Sea Ice Simulator, the first experiments to evaluate the TUV snow model for undoped sea ice, the first experimental results to demonstrate the change in reflectance owing to light absorbing impurities in sea ice and finally the first experiments to evaluate the TUV-snow model for reflectivity calculations for light absorbing impurities in sea ice.*"

2.30 Personal preference, and may be disagreed by the editorial team, but this list of aims feels very wordy. Could it be bulleted?

The list of aims has now been removed following similar comments also from the second referee.

7.13 Extra space needed.

An extra space has been added.

9.8: Sentence currently doesn't make sense, too many "for smalls"?

The sentence has been changed to read "Grenfell et al. (2011) showed that for small amounts of black carbon the mass loading is directly proportional to the absorbance measured by the integrating sandwich spectrometer."

10.9 *"with a", not in a?*

Agreed, "in a" has been changed to "with a"

Reply to anonymous referee 2

The authors would like to thank the referee for their comments on the paper "Optical properties of laboratory grown sea ice doped with light absorbing impurities (black carbon)."

Changes made to the paper based on their review are detailed below on a point-by-point basis:

Major concerns:

1. The paper is not particularly well written. I find numerous instances where the writing is sloppy and imprecise. I will attempt to point them out in my minor comments below, but the manuscript could be dramatically improved if some attention were given to the writing.
The paper has been reviewed to sharpen-up the writing and improve the manuscript.

2. There seems to be a mismatch between the title and the stated objectives. The title suggests the point of the paper is to present the optical properties of laboratory grown sea ice containing black carbon. The abstract, however, starts by suggesting the reader should expect a manuscript detailing the validation of a radiative transfer model. P. 1 lines 1-4 are really not clear what this manuscript is setting out to do.
The title of the paper has been changed to include radiative-transfer modelling and now reads: "*Optical properties of sea ice doped with black carbon- An experimental and radiative-transfer modelling comparison*".

The abstract has also been completely rewritten.
"*Radiative-transfer calculations of the light reflectivity and extinction coefficient in laboratory generated sea ice doped with and without black carbon demonstrate that the radiative transfer model TUV-snow can be used to predict the light reflectance and extinction coefficient of sea ice typical of first year sea ice containing typical amounts of black carbon and other light absorbing impurities. The experiments give confidence in the application of the model to predict albedo of other sea ice fabrics.*

Sea ices, ~30 cm thick, were generated in the Royal Holloway Sea Ice Simulator (~2000 L tanks) with scattering cross-section measured between 0.012 and 0.032 m² kg⁻¹ for four ices. Sea ices were generated with and without ~5 cm upper layers containing particulate black carbon. Nadir reflectances between 0.60 and 0.78 where measured along with extinction coefficients of 0.1 to 0.03 cm⁻¹ (e-folding depths of 10-30 cm) at a wavelength of 500 nm. Values were measured between light wavelengths of 350 and 650 nm. The sea ices generated in the Royal Holloway Sea Ice Simulator were found to be representative of natural sea ices.

Particulate black carbon at mass ratios of ~75, ~150 and ~300 ng g⁻¹ in a 5 cm ice layer lowers the albedo to 97%, 90%, and 79% of the reflectivity of an undoped ``clean'' sea ice (at a wavelength of 500 nm)."

3. I am not entirely comfortable with the nature of the comparisons being made between the observations and the model. There seems to be some circularity here. In the abstract (lines 6 – 7) it is stated that measured apparent optical properties (albedo and extinction) are used to derive inherent optical properties (scattering and absorption cross-sections) "using the model". It is not at all clear what this means. Then lines 10 -12 state that

light extinction (e-folding depth) is calculated using the model and the IOPs that were derived directly from AOPs (lines 6 -7)? This sounds rather circular- like saying that the measurements are used to define the inherent optical properties of the domain (using the model), which are then fed back into the model to produce apparent optical properties, for comparison with the measured AOPs. Well, I would hope those would agree!

The abstract has been re-written to be clearer

Page 2 line 30 states that it is the third objective of this work to use measured [apparent] optical properties to recreate the irradiance within the sea ice using the TUV-snow radiative transfer model and compare modelled and measured values. To me, this says that the objective is to use the observations to infer IOPs appropriate for input for the model, and to then compare modelled and measured AOPs. I don't think this is a legitimate comparison! The model is being forced to agree with the observations! There is no independent comparison here. The further discussion on p. C2 12 (lines 2 – 4) reinforces this circularity.

The objectives have been removed as they caused confusion.

Also there is no circularity in the procedure presented here; we are demonstrating we can reproduce our experimental data with modelled data and then perturb the experiment (with black carbon) and continue to reproduce the experimental data with the model. Furthermore using the reviewer's (and Mobley's) nomenclature:

- The AOPs of the sea ice are measured and modelled to determine values of the IOPs
- To determine how well the model AOPs fit the measured AOPs we compare the modelled AOPs with the measured AOPs
- We perturb the experiment with the addition of black carbon and measure AOPs. We than compare modelled and measured AOPs

Thus we demonstrate that:

1) We can reproduce our experimental AOPs (n.b. we use *e*-folding depth and albedo, most studies only use albedo thus our system is more constrained) by modelling IOPs of pure ice. The TUV-snow radiative-transfer model can be used to describe the radiative-transfer in and above the sea ice

2) We can perturb the experimental system with a known amount of a known absorber and reproduce the experimental results with our model. Note the system is constrained by amount, size and MAC of an absorber and these cannot be used as modelling parameters such as those used in other studies.

4. Use of upwelling radiance to determine e-folding depth in finite-depth domain with forward peaked scattering phase function? If I understand correctly, the e-folding depth is calculated from the measurement of upwelling radiance. I would expect the measurement of e-folding depth in this relatively thin (30 – 50 cm) ice block to be biased low, but measuring the upwelling radiance makes it only worse. Take the limiting case of an upwelling radiance measurement immediately above the ice-water interface. I would expect it to be near zero, whereas the downwelling radiance would be non-zero. The e-folding depth from those two different measurements should be quite different.

The following text has been added to the manuscript to clarify this:

"*At each depth drilled the same fibre optic is inserted into the hole and the light intensity (upwelling radiance) measured via an Ocean Optics spectrometer. In an optically thick sea ice the measurement of either up or downwelling light for e-folding depth is not important as has been shown by France et al. 2012.*"

And:

"Measurements used to calculate the e-folding depth are only conducted in the middle of the ice as the irradiance profile changes rapidly at the air-ice and ice-water boundary (a good example shown in King et al. 2005). The calculation of an e-folding depth from the modelled downwelling irradiance was calculated from similar depths as the experimental ice. The modelled ice had the same thickness and underlying tank radiance field as the experiment"

The authors are well aware of the boundary effects that occur at the air-ice and ice-water interfaces, therefore no measurements were performed near the upper or lower ice boundaries, as we (King, et al 2005) have previously shown the irradiance profile changes rapidly at these edges. The optically "thin" sea ice would not produce an asymptotic value of the *e*-folding depth in the experiments measured but produce a phenomenological value for this particular experiment. Thus our use of radiative-transfer modelling to reproduce the reflectance and the *e*-folding depth to determine values of σ_{abs}^{+} and σ_{scatt} which are not phenomenological. It should be remembered that sea ice, like snow, is a diffusing media and that in an optically thick sea ice the measurement of either up or downwelling light for *e*-folding depth is not important as has been shown by France et al. 2012 for optically thick media. It should also be noted that the limiting case mentioned by the referee for the experimentally measured upwelling radiance in this study would not be zero as the bottom of the tank is reflective and the radiative transfer modelling included the measured reflective bottom. It has been shown in France et al. 2012 that the angle at which measurements of the *e*-folding depth are made in an optically diffuse media has no effect on the resultant values.

5. Confusion between radiance and irradiance? I thought that the ratio of upwelling nadir radiance to downwelling nadir radiance was being measured, but on page 12 line 13 it sounds like the measurement is ratio of upwelling irradiance to downwelling irradiance. Is there confusion here between "radiance" and "irradiance"? They are radiometrically distinct quantities and should not be interchanged. Additionally, p. 20 line 30 states that the reflectance of the laboratory grown (not 'gown') ice is considerably larger than first year ice, and resembles a reflectance closer to multi-year ice. Does this statement mean that the spectral ratio of upwelling to downwelling radiance (as far as I can tell, the only optical property measured above the ice) is being compared to spectral albedos published in the literature? Here again, I think it is possible there may be some confusion between radiance and irradiance? Or is the model being used to estimate the albedo of the ice which is then being compared to the albedos of ˇ natural ice? What natural ice measurements are being used in this comparison? Also, it would be helpful to present the measured spectral reflectivity of the tank, since it possibly matters so much.
The comparison to literature albedos have been removed as the measurements of the albedo reported in literature would have been performed under clear skies and therefore the referee is right to point out these are incomparable to the measurements taken of the laboratory grown sea ice under diffuse conditions. The manuscript has been checked that the terms radiance and irradiance have been used correctly throughout.
The spectral nadir reflectance of the tank bottom has been added to the supplementary information and a reference to this added in the text.

6. Figure 7 shows wavelength-dependent absorption cross-section derived from reflectance and e-folding depth data from the four runs, with no BC. I am concerned about the interpretation of these data. These curves don't really look like chlorophyll absorption spectra to me. Chlorophyll typically has absorption maxima at 430 – 450 nm and 640 - 670 nm. How was the absorption of water and ice represented in the model? Is it possible there was some error in representing the ice and/or the brine, and these spectra, which look similar in nature to the absorption of water?

The absorption spectra of chlorophyll from Bricaud et al. (2004) and chlorophyll in ice from (Mundy et al. 2011) have been added to figure 7 (now figure 9) to demonstrate the algae absorption. In previous experiments, not reported here, we have observed algae at visible concentrations in the tank.

Minor points:

P. 1 L 14: As pointed out by a different reviewer in a short comment, the last line of the abstract states that "albedo is reduced by" as much as 97%. This cannot be accurate!
The wording has been corrected to read "*to*" instead of "*by*"

p. 1 L 22: What is the "TUV-snow radiative transfer model for sea ice"? I am not familiar with it, and I find it rather confusing that it is a "snow" model for "sea ice". What does TUV stand for?
Further explanation of the TUV-snow model has been including here for clarity: "*The following study presents the first data from the RHUL sea ice simulator used to validate the Tropospheric ultraviolet and visible (TUV)-snow radiative-transfer model for use with sea ice. The TUV-snow model is a coupled atmosphere-snow radiative-transfer model, described in detail by Lee-Taylor and Madronich (2002). The model has been used multiple times for investigations of radiative-transfer in snow (e.g. King et al. (2005), France et al. (2011), France et al. (2012), Reay et al. (2012)) and has also been adapted for use with sea ice (e.g. King et al. (2005), Marks and King (2013), Marks and King (2014) and Lamare et al. (2016)). The model has previously been experimentally validated for photochemistry in snow by Phillips and Simpson (2005) but it has not been experimentally validated for sea ice.*"

The reference to Lee-Taylor and Madronich (2002) is a full description of the model. TUV stands for tropospheric ultraviolet and uses the DISORT code of Stamnes et al. (1988). These are standard, freely available tools of radiative-transfer studies.

p.2 L2: Here the authors mention that the sea ice simulator has "not been experimentally validated for sea ice." If that is an objective of this manuscript then it should appear perhaps in the title, and probably in the abstract. The paper is a bit diffuse because it seems to have many different objectives, as listed at the bottom of p. 2.
The title of the paper has now been changed to reflect the main objective of the paper and the list of objectives has been removed from the paper and instead the section restructured to portray the main aims of the paper.

p.2 L 14-15: It is not clear why validating the TUV-snow model just for a single type of sea ice, grown under particular circumstances, and a single absorber, in this case BC, necessarily means the model can be used "confidently" for other sea ice types and absorbers. For instance, I can imagine that ice grown with very few scatterers could have much smaller optical depth, and perhaps would be a different modelling problem than the one examined here.
The suggestion the model could be used "confidently" has been toned down, with the text changed from "*If the radiative-transfer modelling with TUV-snow can reproduce the laboratory grown ice with absorbing impurities it will allow the model to be used confidently for other sea ice types and absorbers.*" to read "*The work presented here will demonstrate that radiative-transfer modelling with TUV- snow (Lee-Taylor and Madronich, 2002) model can reproduce laboratory grown ices with differing fabrics with a range of mass ratios of light absorbing impurities. Such a validation will give confidence to others in the calculations of TUV-snow for other sea ices and other light absorbing impurities.*"

The TUV-snow model has been applied to ablating sea ice (King et al. 2005) and the sea ice described in Grenfell and Maykut (1977) in Marks et al. (2013) and so has been used for other sea ice types. To the authors knowledge very few other radiative-transfer models of sea ice have been validated in a laboratory experiment, for doping with light absorbing impurities and whilst such experiments cannot cover all scenarios it gives more confidence than in an unvalidated model. If all scenarios could be validated by experiments then a model would not be required. It is the author's assertion that a model that has been successfully validated with realistic laboratory experiments is more useful than a model that has not.

p.3 L 9: "temperature" is "higher/lower", not "warmer/cooler"
The sentence referring to "warmer Polar temperatures" has been rewritten based on different comments from the other referee. The text now reads "*The sea ice simulator is designed to replicate a Polar sea ice growth environment under UV and visible wavelengths of solar radiation.*"

Figure 1: I see the tank volume is 2000 litres, but there is no indication of the diameter and depth? They matter, particularly in regards to the exchange of salt between the growing ice sheet and the "ocean".
The diameter and depth of the tank were originally stated in section 2.1. For clarity they have also been added to the caption of figure 1.

p.4 L7: does the pump achieve vertical mixing? Are you only worried about temperature stratification? What about salinity stratification?
Yes, the pump achieves vertical mixing and therefore both temperature and salinity will not be stratified, this was the purpose of the pump. The text has now been altered to read: "*To create circulation within the tank, ensuring temperature and salinity stratification does not occur, an Iwaki….*"

p.4 L14: what does "majority of shortwave solar wavelengths" mean? Please clarify.
For clarity this sentence has been restructured to read "*Illumination replicating shortwave solar wavelengths over 350-650 nm is provided with a set of …*"

p. 4 L18: Was the incident light field isotropic? Or just diffuse? It is difficult to create an isotropic light field in the laboratory, but it is also difficult to simulate a diffuse light field that is not isotropic in a model. Just saying they are both diffuse, does not ensure a valid comparison.
The following text has been added to the manuscript "*The radiance, as a function of azimuth and zenith angle within the experiment was checked with a fibre optic probe and a broadband visible wavelength measurement and found to vary by 5-10%*".

p.5 L7: Drilling a hole breaks the horizontal homogeneity of the ice block, could cause additional brine drainage, and does reduce the integrity of the ice, but the authors should be wary of stating that it "destroys the fabric of the ice", as I don't think this is accurate.
The text has been revised from "*destroys the fabric of the ice*" to "*destroys the homogeneity of the ice*"

p.6 L5: what size is the reflector panel? At some size it will reflect significant radiation back to the "sky" (lighting panels and white boards) and enhance the downwelling radiation field, biasing the reflectance. Please state the size of the panel and discuss the possibility of it affecting the measurement of the incident light.

The following text has been added to the paper:

"*During a reflectivity measurement a 30 × 30cm Spectralon panel is added to the diffuse lighting environment above the sea ice. The addition of this panel increases the radiance, L, within the diffuse lighting environment. The Spectralon panel represents 0.66% of the area of the diffuse lighting environment, which is approximately a cube made up of white panels and sea ice (i.e. 6 x 1.5 x 1.5= 13.5 m^2). Treating the diffuse lighting environment above the sea ice as a crude integrating sphere and considering fractional change in radiance, δL/L, after Ball et al. 2013 who suggest $\delta L/L \approx A_{panel}/A_{environment}\rho$. Where A_{panel} is the area of the Spectralon panel, $A_{environment}$ is the area of the diffusing "cube" and ρ is the overall reflectivity of the diffusing cube. A very crude analysis assumes reflectivity of the panel is 1 and the part fraction of the hypothetical integrating sphere is 0. In the limit of a reflective environment $\delta L/L \rightarrow A_{panel}/A_{environment}\rho$ ~0.67%. Thus the overestimation of the radiance (~0.67%) is significantly less than the uncertainty displayed on the measurement of nadir reflectivity displayed in figure 3 and figure 7.*"

p.6 L22: what does it mean that the "e-folding depth . . . is asymptotic"? please clarify. Also, it is not accurate to say "there are no near surface effects". The fact that this is a finite domain means there necessarily will be some surface effects.

The following text has been revised for clarity "*The extinction coefficient and e-folding depth measured in the work presented here is asymptotic (reaches a constant value as shown in King et al. (2005))*"

The asymptotic region is the region where the logarithm of the radiance decreases linearly with depth and the value of the e-folding depth reaches an asymptote or constant value as shown in King et al. (2005), figure 10.

p.7 L17: "proportion"? I think "portion" is intended?

"*Proportion*" has been changed to "*portion*"

p.7 L27: why two (very different!) values for the mass absorption cross-section?

These values for the mass-absorption cross-section were obtained using different comparison materials; acetate and polypropylene sheets. The 0.58 m^{2}g^{-1} value (obtained from using the acetate sheets) has been removed from the text and was an erroneous value left in from an earlier edit for a failed determination. The acetate sheets were unsuitable for these type of measurements.

Table 1: units for density are not g cmˆ3. Also, I am confused about the cross-section units of cmˆ2 kgˆ-1. Cross-sections on previous page are cited in mˆ2 gˆ-1. Those are not equivalent.

Units for density have been changed from g cm^3 to g cm^{-3}. We are keeping nomenclature of Lee-Taylor and Madronich (2002) and the body of our work (e.g. King et al. (2005), France et al. (2011), France et al. (2012), Reay et al. (2012), Marks and King (2013) and Marks and King (2014) in similar units. The units of m^2 kg^{-1} are used for scattering cross-sections, while cm^2 g^{-1} are used for absorption cross-sections, the authors are aware these units are not equivalent.

Fig. 2 Y-axes have different labels should they not both be "Relative spectral absorbance"? I understand the two figures are for different materials, but I think they are intended to be compared, and if that is so then they should have the same label on their y-axes.

The y-axis on both of these figures has been changed to "*Relative spectral absorbance*"

p. 9 L 8 and following. This sentence is cryptic. It needs to be rewritten for clarity.
The sentence has been changed to read "*Grenfell et al. (2011) showed that for small amounts of black carbon the mass loading is directly proportional to the absorbance measured by the integrating sandwich spectrometer.*"

p. 12 L 5: Why is ice density measured and reported? Is it used in the modeling? If so, the way that is used could be important and should be described.
When describing sea ice it is normal to record its mass density (Eicken, 2003) as it can be used to calculate other properties of the sea ice as described by Weeks (2010)

p. 12 L 10 -11: Sentence beginning "The reflectance under. . ." needs to be rewritten for clarity.
Agreed, this sentence was poorly written. The sentence has been changed from "*The reflectance under the ice is the measured, wavelength dependent, nadir reflectance of the bottom of the water filled tank*" to "*The wavelength dependant, nadir reflectance of the water filled tank is measured and included in the model as the under ice reflectance.*"

p. 13 L 4- 5: Higher air temperature should result in slower ice growth. Slower ice growth would be expected to result in less entrainment of brine within the ice. Less brine would be expected to yield fewer and/or smaller brine inclusions, which would then result in reduced scattering.
The authors agree with the referee's logic that a larger value for the temperature of the air would result in slower ice growth, however as stated in the paper the air temperature is kept constant for all experiments.

p. 14 L 3 -4: see comments above about reduced salinity. The data displayed in figures 5 and 8 really should be presented on the same plot; it is very difficult to make the comparison when they are in different figures.
Figures 5 and 8 should appear on the same page of the final manuscript for easy comparison of the figures. The figures were kept separate for clarity as the figure becomes cluttered to read when plotted on one graph. Any adjustment can be made at the proof stage.

p. 18 L 13: No, sea ice is not at its eutectic point, unless it is very cold (about -37 C). When in thermal equilibrium, it is always at its melting point, hence the required equilibrium concentrations of brine and ice.
The reference to sea ice always being at its eutectic point has been removed from the text.

Figure 9: please specify which y-axis corresponds with which curves.
The figure has been changed to make it more obvious which axis corresponds to which curve.

p. 19 L 4 -7 : This relates to a commonly recognized "similarity principle" in radiative transfer.
Reference to the "similarity principle" has been added to the text.

p. 20 L 15, following: does the exchange of seawater in the "ocean" of the simulator correct for salinity variations? I would expect even a 30 cm thick ice cover could affect the salinity of the ocean, but since the dimensions of the tank are not given (other than total volume), it is impossible to estimate the salinity enhancement in the 'ocean' due to freezing of the ice and resulting salt rejection.

The sea ice thickness is kept thin so that the salinity of the water below the sea ice does not get too large to be unrealistic. The salinity of the underlying liquid is measured during ice growth and does increase slightly due to brine expulsion into the water.

p. 21 L 11: Here again, ". . .reduce the albedo of the ice by 97%…" I think this should be ". . .reduce. . . to 97%".
Correct, the text in the manuscript has been changed from "*by*" to "*to*"

p. 21 L 15: "The derived scattering cross-section values are typical of sea ice. . ." what are the derived values being compared to?
The following has been added to the manuscript for comparison "*The derived values of the scattering cross-section are typical of sea ice (e.g. Grenfell and Maykut 1977, Timco and Frederking, 1996, Perovich 1996), while the derived…*"

Reply to S. Doherty

The authors would like to thank S. Doherty for their comment on the paper "Optical properties of laboratory grown sea ice doped with light absorbing impurities (black carbon)."

A (likely) correction to the Abstract: "Particulate black carbon at mass ratios of 75, 150 and 300 ng/g in a 5 cm ice layer lowers the albedo by 97%, 90%, and 79% compared to clean ice at a wavelength of 500 nm." I believe that the authors mean that it "lowers the albedo to (i.e. not "by") 97%, 90% and 79%" – or some other wording adjustment is needed. Lowering it *by* 97% would make for some C1 TCD Interactive comment Printer-friendly version Discussion paper very black ice indeed!

They are correct in their comment on the wording and this has been changed in the revised manuscript to say "*to*" instead of "*by*".

Optical properties of ~~laboratory grown~~ sea ice doped with ~~light absorbing impurities (black carbon)~~ carbon- An experimental and radiative-transfer modelling comparison

Amelia A. Marks[1], Maxim L. Lamare[1], and Martin D. King[1]

[1]Department of Earth Sciences, Royal Holloway University of London, Egham, Surrey, TW20 0EX, UK.

Correspondence to: Martin King (M.King@rhul.ac.uk)

Abstract. ~~Sea ice radiative-transfer models are of great importance for prediction of future sea ice trends but they are limited by uncertainty in models and requirement for evaluation of modelled irradiance data against measured irradiance data. Presented here are the first results from the Royal Holloway sea ice simulator used to evaluate the output of the~~

Radiative-transfer calculations of the light reflectivity and extinction coefficient in laboratory generated sea ice doped
5 with and without black carbon demonstrate that the radiative transfer model TUV-snow ~~radiative-transfer model against the optical properties from the simulated sea ice. The sea ice simulator creates a realistic sea ice environment where both optical (reflectance and light penetration depth (-folding depth)) and physical (temperature, salinity, density) properties of a~~ can be used to predict the light reflectance and extinction coefficient of sea ice typical of first year sea ice containing typical amounts of black carbon and other light absorbing impurities. The experiments give confidence in the application of the model to predict
10 albedo of other sea ice fabrics.

Sea ices, $\sim$30 ~~cm thick sea ice can be monitored and measured. Using albedo and -folding depth data measured from simulated sea ice , scattering and absorption cross-sections of the ice are derived using the TUV-snow model. Absorption~~ cm thick, were generated in the Royal Holloway Sea Ice Simulator ($\sim$2000 L tanks) with scattering cross-sections ~~for the ice are highly wavelength dependent, suggesting the addition of a further absorbing impurity in the ice matching the absorption spectrum of
15 algae.~~

~~Scattering cross-sections were wavelength independent with values ranging from~~ measured between 0.012 and 0.032 ~~cm~~ $m^2 \, kg^{-1}$ for ~~different ice created in the simulator. Reflectance and light penetration depth~~ four ices. Sea ices were generated with and without $\sim$5 cm upper layers containing particulate black carbon. Nadir reflectances between 0.60 and 0.78 where measured along with extinction coefficients of 0.1 to 0.03 cm^{-1} (*e*-folding ~~depth) of sea ice is calculated from the derived values of the
20 scattering and absorption cross-section using the TUV-snow model within error of the experiment. The model is also shown to replicate ice optical properties for sea ice with an extra layer doped with black carbon, well within error of the experiment~~ depths of 10–30 cm) at a wavelength of 500 nm. Values were measured between light wavelengths of 350 and 650 nm. The sea ices generated in the Royal Holloway Sea Ice Simulator were found to be representative of natural sea ices.

Particulate black carbon at mass ratios of $\sim$75, $\sim$150 and $\sim$300 ~~ng~~ ng g^{-1} in a 5 cm ice layer lowers the albedo ~~by~~ to 97%,
25 90%, and 79% ~~compared to clean ice~~ of the reflectivity of an undoped "clean" sea ice (at a wavelength of 500 nm).

1

1 Introduction

Rapid decline of sea ice in the Arctic is often seen as a bellwether for modern day climate change (e.g. IPCC (2013)). Model predictions of future sea ice extent have a large degree of uncertainty (e.g. IPCC (2013)). Accurate representation and recreation of the optical and physical properties of sea ice is essential to develop accurate models of sea ice. The Royal Holloway (RHUL) Sea Ice Simulator facility aims to create a realistic sea ice within a controlled environment with the ability to monitor both the physical (temperature, salinity and density) and optical (nadir reflectivity and extinction coefficient) properties of the sea ice. The results from which can be used to evaluate sea ice models.

The following study presents the first data from the RHUL sea ice simulator used to validate the Tropospheric ultraviolet and visible (TUV)-snow radiative-transfer model for use with sea ice. The TUV-snow model is a coupled atmosphere-snow radiative-transfer model, described in detail by Lee-Taylor and Madronich (2002). The model has been used multiple times for investigations of radiative-transfer in snow (e.g. King et al. (2005), France et al. (2011), France et al. (2012), Reay et al. (2012)) and has also been adapted for use with sea ice (e.g. King et al. (2005), Marks and King (2013), Marks and King (2014) and Lamare et al. (2016)). The model has previously been experimentally validated for photochemistry in snow by Phillips and Simpson (2005) but it has not been experimentally validated for sea ice.

The TUV-snow model will be evaluated by comparing measured optical properties (reflectance and extinction coefficient) of sea ice grown in a laboratory to TUV-snow model radiative-transfer calculations for a sea ice with the same properties. Secondly, the model will be evaluated by comparing measured nadir reflectance with light absorbing impurities in the laboratory sea ice to radiative-transfer calculations with the same light absorbing impurities in the sea ice, namely black carbon and algae.

Sea ice typically contains impurities such as black carbon, sediment and algae (e.g. Perovich (1996)). Black carbon is an efficient absorber of solar radiation (e.g. Mitchell (1957); Highwood and Kinnersley (2006); Hansen and Nazarenko (2004); Jacobson (2001); Ramanathan and Carmichael (2008); Bond et al. (2013)) and its deposition onto, or incorporation into, sea ice has been shown through modelling calculations to decrease the surface reflectance of the sea ice, increasing melt rates (e.g. Grenfell et al. (2002); Jacobson (2004); Light et al. (1998); Ledley and Thompson (1986); Goldenson et al. (2012); Holland et al. (2012); Marks and King (2013, 2014)). To evaluate the TUV-snow model with black carbon, a commercial black carbon is added to a 5 cm surface layer of 30–50 cm thick sea ice created in the laboratory in mass-ratios of 0, 75, 150 and 300 ng g^{-1} and the nadir reflectance of sea ice measured. The experimental reflectivity is compared to a calculated reflectivity using the TUV-snow model, for the same black carbon mass-ratios. The work presented here will demonstrate that radiative-transfer modelling with TUV-snow model (Lee-Taylor and Madronich, 2002) can reproduce laboratory grown ices with differing fabrics with a range of mass-ratios of light absorbing impurities. Such a validation will give confidence to others in the calculations of TUV-snow for other sea ice types and other light absorbing impurities.

Previous research on the effects of black carbon on sea ice optical properties have used radiative-transfer calculations and global climate model simulations. To the authors' knowledge there are no laboratory or field studies examining the effects of

added black carbon on reducing sea ice reflectance. A related study by Hadley and Kirchstetter (2012) carried out successful laboratory experiments on artificial snow investigating the effects of black carbon on snow reflectance. The results from Hadley and Kirchstetter (2012) were used to validate the Snow, Ice and Aerosol radiation (SNICAR) model (Flanner et al., 2007) used in the 2013 IPCC report (IPCC, 2013). Similarly, Brandt et al. (2011) investigated the effect of black carbon on albedo of artificial snowpacks using snowmaking machines, showing a good match between measured values and albedos calculated from ~~radiative transfer~~ radiative-transfer modelling. Peltoniemi et al. (2015) measured the effect on snow bi-directional reflectance owing to additions of ~~Chimney~~ chimney soot, volcanic sand, and glaciogenic silt, demonstrating how snow metamorphism caused by the addition of these particles ~~and the subsequent impact~~ subsequently impacted on the albedo.

The study presented here ~~are~~ includes the first experiments with the Royal Holloway Sea Ice Simulator, the first experiments to evaluate the ~~TUV snow model for~~ TUV-snow radiative-transfer model for calculations of extinction coefficient and reflectivity of undoped sea ice~~and the first attempt to compare measurements to calculations using a radiative transfer model of nadir~~, the first experimental results to demonstrate the change in reflectance owing to ~~black carbon~~ light absorbing impurities in sea ice ~~.~~ ~~There are five overall aims of the study: firstly to grow realistic artificial sea ice; secondly to characterise optical and physical properties of the sea ice; thirdly to use measured optical properties to recreate the irradiance within the sea ice using the TUV-snow radiative transfer model and compare modelled and measured values; fourthly to create a 5 cm layer of sea ice doped with black carbon with mass-ratios of 0, 75, 150 and 300 ng g^{-1} and measure the reflectance; finally to compare the measured reflectance with black carbon in the surface layer of sea iceto calculations with the~~ finally the first experiments to evaluate the accuracy of the TUV-snow model for reflectivity calculations for light absorbing impurities in sea ice.

Throughout the paper the term "experimental" refers to experiments with laboratory grown sea ice using the sea ice simulator described in section 2.1, with results being referred to as "measured" values. The term "modelled" refers to calculations from the TUV-snow radiative-transfer model, the results from which are referred to as "calculated" values.

2 Experimental method

The following sections will describe the design of the sea ice simulator (section 2.1), the characterisation of both the optical and physical properties of the ~~simulated~~ laboratory ice (section 2.2) and the creation of sea ice doped with black carbon particles (section 2.3).

2.1 Sea ice simulator design

The sea ice simulator is ~~a large scale, UK-based, laboratory sea ice tank~~ designed to replicate ~~warmer polar temperatures, the ocean and~~ a Polar sea ice growth environment under UV and visible wavelengths of solar radiation. Previous experiments with sea ice simulators have been carried out by, for example, Light et al. (2015); Buist et al. (2011); Papadimitriou et al. (2003); Haas et al. (1999); Polach et al. (2013); Hare et al. (2013); Grenfell and Perovich (1981). The set up of the simulator is shown in figure 1. The simulator is housed in a refrigerated shipping container (11.95 m length × 2.56 m high × 2.29 m width) which can be temperature controlled from –25°C to 25° C. The air temperature within the container varies by $\pm 1°C$ although

Inside the container sea ice is formed in a 2000 L polyethylene cylindrical white plastic tank (1.32 m high $\times$ 1.39 m diameter) placed on insulated pallets. Following the approach of Perovich and Grenfell (1981) a cylindrical design is utilised for the tank to help avoid mechanical stress at particular locations. A 1 cm insulating layer of black neoprene also surrounds the tank sides. A metal Unistrut frame surrounds the tank to further improve structural integrity. Black wooden boards, painted with mould resistant paint, are fixed around the Unistrut structure with 3 cm thick polystyrene insulation fitting between the wooden boards and the tank.
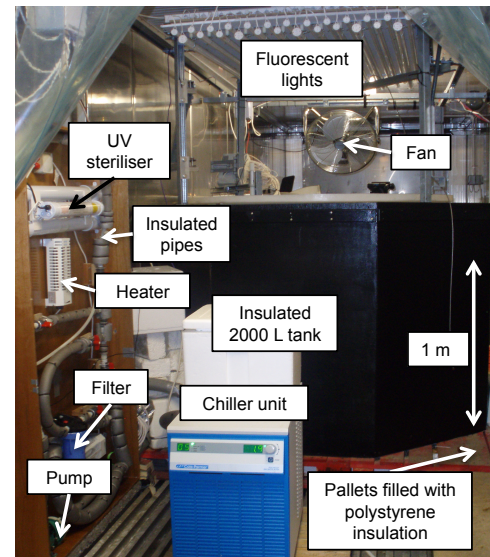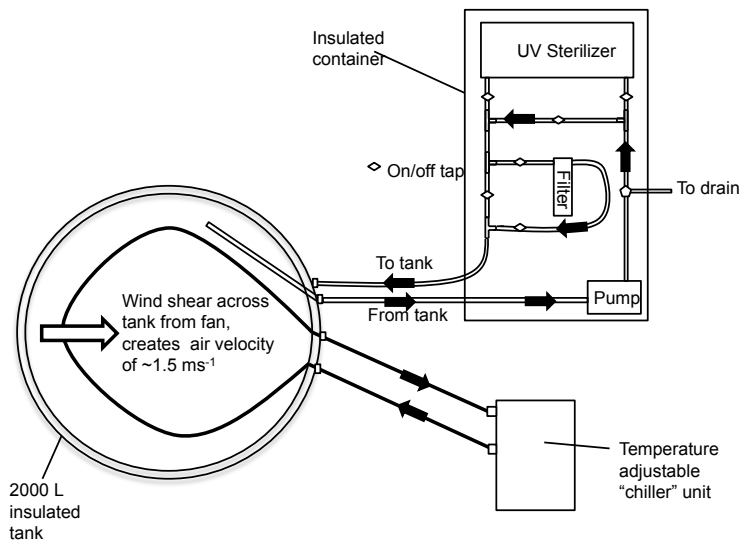

Figure 1. Plan of the sea ice simulator showing the 2000 L cylindrical tank (1.32 m high $\times$ 1.39 m diameter) in plan view and water conditioning unit in horizontal view and annotated photo of the facility. A closed pipe runs around the base of the tank connected to a heater unit circulating a water and glycol mixture gently warming the base of the tank. Water is circulated around the tank by a pump in an insulated container and also passed through a UV sterilser steriliser and particulate filter. Note the diffusing hood and insulation have been stripped away for clarity in the photo.

The tank is filled with a solution of Tropic Marine (Atkinson and Bingman, 1997) and giving water with a salinity of 32 PSU, representing Arctic ocean salinity (Boyer et al., 2013). Tropic Marine is a synthetic sea salt mixture for aquaculture containing over 70 chemical elements in typical natural concentrations representative of the ocean with the notable exception of nitrate and phosphate, to inhibit algae growth. Atkinson and Bingman (1997) show the concentrations of major cations and anions of Tropic Marine are within 10% of seawater. Previous sea ice simulators use either sodium chloride or synthetic sea salt mixtures similar to Tropic Marine (e.g. Krembs et al. (2001), Mock et al. (2002), Papadimitriou et al. (2003) and Hare et al. (2013)).

To create circulation within the tank, ensuring temperature and salinity stratification does not occur, an Iwaki MD-10 pump circulates water at ∼10 L min^{-1} at the base of the tank, as shown in figure 1. The circulated water is also pumped through a 10 μm filter to remove any particulate impurities and a UV steriliser to prevent algae growth.

Sea ice grows from surface cooling of a salt water body (Weeks, 2010). To ensure even and realistic ice growth in the tank
5 (from the surface, downwards) a closed pipe is run around the bottom of the tank, connected to a heater unit. The heater unit contains a solution of water and pure ethylene glycol (in a 1:1 ratio) which is pumped around the pipe at a constant temperature (0°C), to warm the base of the tank and preventing freezing. Figure 2 demonstrates that the temperature of the water beneath the sea ice is not thermally stratified, ice temperature decreases linearly through the ice with depth and the ice surface temperature is at a constant −15°C.
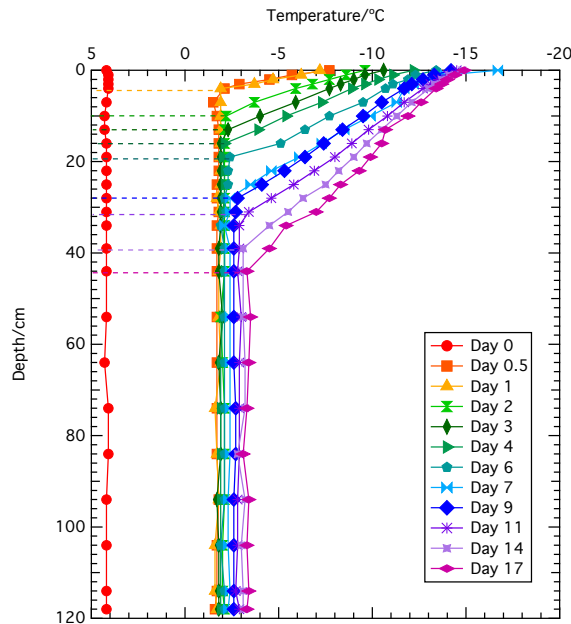10 ~~Illumination replicating the majority of~~

Figure 2. Temperature profiles through ice during ice growth. The top section, showing a linear increase in temperature, shows measurements from the ice, while the bottom section, with a constant temperature, shows measurements from the under-ice seawater, demonstrating the water is not thermally stratified.

Illumination replicating shortwave solar wavelengths (over 350–650 nm)is provided with a set of twenty Daystar daylight simulation fluorescent tubes and five sun-bed ultraviolet tube lights (peak illumination wavelength of ∼350 nm, 40 nm FWHM). Measurements of reflectance of the sea ice is a relative measurement, (i.e. the quotient of reflected radiance ~~to incident radiance or~~ of sea ice to reflected radiance from a reflectance standard) thus the intensity-spectrum of the lamp does not have to match
15 the solar spectrum. The lights are evenly distributed directly above the tank to provide a diffuse illumination source. The light

is further diffused by opaque white boards placed around the edges of the tank. Diffuse lighting was used to simplify the measurement of extinction coefficient and provide a useful reflectance product. The radiance, as a function of azimuth and zenith angle within the experiment was checked with a fibre optic probe and a broadband visible wavelength measurement and found to vary by 5-10%. The short term variability of the lamps was less than 0.1% (after an initial warm-up) on the timescale

5 of the measurement of reflectivity or e-folding depthand provide a useful reflectance product. Note that both the value of nadir reflectance (relative to a Spectralon panel) and light penetration depth are not dependent on the illumination irradiance providing the irradiance does not change during the measurement. Figure 3 shows the change in ice nadir reflectance during ice growth and the day-to-day reflectance stability of the optically thick ice.
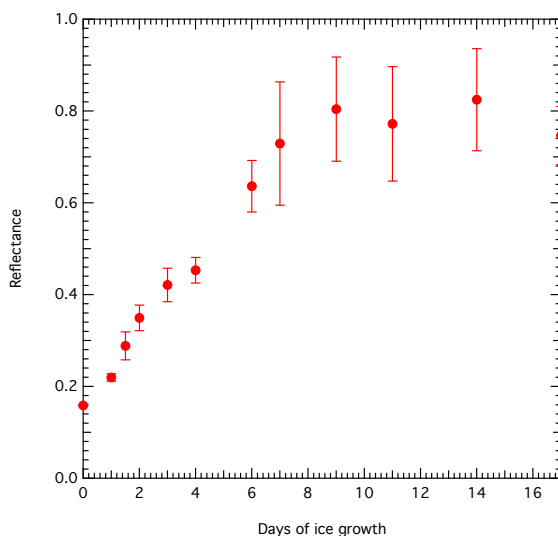

Figure 3. Reflectance of sea ice during ice growth and the day-to-day reflectance stability of the potentially optically thick ice (day 10 onwards).

2.2 Creation and characterisation of sea ice

10 To create sea ice an air temperature inside the container of $\sim -15°$C is maintained. Cold air is circulated within the container with fans. An additional air fan, attached to the ceiling, blows cold, ambient air at the water surface $,(110\,\text{m}^3\,\text{min}^{-1})$ increasing the heat flux from the ice surface, quickening ice formation and assisting the production of columnar ice (Weeks, 2010).

Sea ice is grown in the simulator for $\sim$17 days producing ice with a thickness of $\sim 30\,cm\sim30\,\text{cm}$. Temperature depth profiles and nadir reflectance of the ice were measured daily during growth (described in sections 2.2.2 and 2.2.5 respectively).

15 Light penetration depth (-folding depth) The extinction coefficient is measured at the end of the experiment as it destroys the fabric homogeneity of the ice (described in section 2.2.6). The -folding depth is the distance over which light intensity reduces to $\frac{1}{e}$ of its initial value.

2.2.1 Characterisation of sea ice physical properties

2.2.2 Temperature profiles

Temperature profiles through the sea ice are recorded daily during ice growth to give an indication of sea ice thickness and ensure that temperature stratification does not occur within the underlying seawater. The temperature is recorded via a series of thermocouples, as used by Rabus and Echelmeyer (2002); Johnston and Timco (2002); Nomurai et al. (2006). Calibrated type T thermocouples are inserted into a thin plastic sleeve and then a white ~~polypropolyne~~ polypropylene pole at regular depths (every 2 cm) into the water and then frozen in place during ice formation. The precision on all the thermocouples at −15°C was measured as ±0.2°C. Temperature of sea ice decreases from the surface to the base; ice thickness can be determined from the point where the temperature becomes constant with depth ~~, as this~~ which can be assumed to be seawater, as shown in figure 2.

2.2.3 Determining sea ice properties by ice coring

Cores of the ice are taken to determine sea ice properties at the conclusion of the optical experiments (section 2.2.4). The corer design was based on a CRREL report by Rand and Mellor (1985). Cores are photographed, divided into ∼5 cm sections and their dimensions and mass measured to derive density. Salinity is measured after melting using a Fisher Scientific seawater refractometer (cross-calibrated with an accurate ion conduction probe).

2.2.4 Characterisation of sea ice optical properties

2.2.5 Measuring reflectance

The nadir reflectance of the sea ice is measured daily during ice growth until the value became constant (taking between 6 and 12 days). Reflectance becomes constant once a sufficient ice thickness is reached that the ~~underlying water no longer affects reflectance measurements, thus the reflectance of ice alone is measured~~ increasing ice thickness does not change the measured reflectivity. Upwelling radiance from the ice is measured via an optical lens connected to a 400 μm xsr fibre optic coupled to an Ocean Optics USB 2000+ spectrometer (wavelength range: 200-850 nm, resolution: 1.5 nm FWHM, signal:noise 250:1). The optical lens is situated ∼40 cm above the sea ice surface at nadir with a view footprint covering a circular area ∼315 cm^2. The footprint is an order of magnitude larger than any surface feature on the sea ice.

To convert ice surface radiance measurements to reflectance the radiance of light from the sea ice surface measured at nadir is ratioed to the radiance from a reference ~~quasi-Lambertian~~ Lambertian reflector at nadir (a Spectralon panel) measured in the same location but raised 5 mm above the ice surface and under identical illumination as the sea ice.

During a reflectivity measurement a 30 cm × 30 cm Spectralon panel is added to the diffuse lighting environment above the sea ice. The addition of this panel increases the radiance, L, within the diffuse lighting environment. A very conservative estimate of the effect on the measurement of the reflectivity can be calculated by analogy to an integrating sphere. The

Spectralon panel represents 0.66% of the area of the diffuse lighting environment, which is approximately a cube made up of white panels and sea ice (i.e. 6×1.5 m $\times 1.5$ m $= 13.5$ m^2). Treating the diffuse lighting environment above the sea ice as a crude integrating sphere and considering fractional change in radiance, $\frac{\delta L}{L}$, after Ball et al. (2013) who suggest $\frac{\delta L}{L} \approx \frac{A_{panel}}{A_{environment}\rho}$. Where A_{panel} is the area of the Spectralon panel, $A_{environment}$ is the area of the diffusing "cube" and ρ is the overall reflectivity of the diffusing cube. A very crude analysis assumes reflectivity of the panel is 1 and the part fraction of the hypothetical integrating sphere is 0. In the limit of a reflective environment $\frac{\delta L}{L} \rightarrow \frac{A_{panel}}{A_{environment}\rho} \sim 0.67\%$. Thus the overestimation of the radiance ($\sim 0.67\%$) is significantly less than the uncertainty displayed on the measurement of nadir reflectivity displayed in figure 3 and figure 7.

2.2.6 Measuring ~~folding depth~~extinction coefficient

At the completion of the experiment the ~~light penetration depth (~~extinction coefficient and e-folding depth are measured. The e-folding depth ~~) is measured. The~~ is the distance over which light intensity reduces to $\frac{1}{e}$ of its initial value and is the reciprocal of the extinction coefficient. The e-folding depth is reported in addition to the extinction coefficient. The sea ice e-folding depth and extinction coefficient is measured by drilling a single hole gradually through the ice in ~ 5 cm increments with a sharp drill. At each depth drilled the same fibre optic is inserted into the hole and the light intensity (upwelling radiance) measured via an Ocean Optics spectrometer. In an optically thick sea ice the measurement of either up or downwelling light for e-folding depth is not important as has been shown by France and King (2012). The hole is a tight fit around the fibre but a thin, light diffusing disk, of white PTFE is also placed around the fibre at the ice surface to minimise any stray light entering the hole without altering the light field near the hole.

Simultaneously to the light intensity in the hole being measured (I_{raw}) the light intensity of another fibre optic inside a diffusing PTFE container at the ice surface was measured (I_{ref}) to account for any change in the intensity of the fluorescent lights. The relative light intensity, I_z , at depth, z, is then calculated using equation 1.

$$I_z = \frac{I_{raw(z)}}{I_{ref}} \tag{1}$$

The e-folding depth, ϵ, is calculated using equation 2, where I_z is the relative intensity at a depth, z, and $I_{z'}$ is intensity at the shallowest depth, z'. From the measured light intensity ~~values~~ the e-folding depth is calculated by fitting an exponential curve through I_z versus z data.

$$\frac{I_z}{I_{z'}} = e^{-\left(\frac{(z-z')}{\epsilon}\right)} \tag{2}$$

The extinction coefficient, k, is than calculated as the reciprocal of the e-folding depth~~measured in this work is asymptotic as~~.

Measurements used to calculate the e-folding depth are only conducted in the middle of the ice as the irradiance profile changes rapidly at the air-ice and ice-water boundary (a good example shown in King et al. (2005)). The calculation of an

e-folding depth from the modelled downwelling irradiance was calculated from similar depths as the experimental ice. The modelled ice had the same thickness and underlying tank radiance field as the experiment. The extinction coefficient and *e*-folding depth measured in the work presented here are asymptotic (reaches a constant value as shown in King et al. (2005)) as the light field to the sea ice is diffuse and thus there are no near surface effects as found frequently in fieldwork (e.g. Reay et al. (2012) and references therein).

2.3 Creation of black carbon doped sea ice

Once the sea ice has grown to ∼30 cm thick (∼3 weeks of ice growth) 75 L (equivalent to a ∼5 cm layer) of chilled seawater doped with a known concentration of black carbon (described in section 2.3.1) is added to the surface and frozen in place forming a 5 cm black carbon bearing ice layer. Black carbon is placed within a 5 cm surface layer of the artificial ice to replicate black carbon entrainment into sea ice following melting of overlying snow as described by Grenfell et al. (2002) and Doherty et al. (2010). The new 5 cm layer of black carbon bearing seawater is left to freeze for three days and the reflectivity of the new sea ice surface then measured daily over a week. The sea ice is then cored and density and salinity measured down the core to record the physical ice structure before and after the black carbon bearing layer is added.

At completion of the experiment the ice is melted and water is purified by filtration through a 1 μm Purtex filter to remove black carbon particulates. If any black carbon particulates were to remain the concentration would be negligible as it would be diluted by 2000 L of sea water (a dilution factor of ∼30). The whole process is repeated with other black carbon concentrations in the 5 cm layer giving a total of four mass loadings; ∼75 ng g^{-1}, ∼150 ng g^{-1} and ∼300 ng g^{-1} and a blank run with 0 ng g^{-1} of black carbon. ~~Between runs the tank is periodically bleached~~ The sea ice was melted and the resulting seawater was treated with aqueous hypochlorous acid (HOCl) and filtered between experimental runs to remove any algae that may have grown. No algae was visible to the naked eye.

2.3.1 Creating atmospherically representative black carbon

To create the aqueous black carbon solutions a method from Clarke (1982) is adapted. The black carbon used, Monarch 120, is produced by Cabot Corporation to replace the discontinued Monarch 71 used by Grenfell et al. (2011). Approximately 1 g of the black carbon is added to a solution of 800 ml of pure water and 200 ml isopropanol (isopropanol aids dispersal of the black carbon in the concentrated solution) (Clarke, 1982). The solution is then placed in an ultrasonic bath for 2 hours to ensure the black carbon is fully dispersed and to break up conglomerated lumps. The solution is then suction filtered through 2 μm Nuclepore membrane filters followed by 0.8 μm Nuclepore filter to remove larger particles and ensure the final solution is representative of atmospheric black carbon i.e. particle diameter <0.8 μm (Clarke, 1982). The mass loading of black carbon in the solution is determined gravimetrically (i.e. by evaporating and weighing a ~~proportion~~ portion of the black carbon solution). Two black carbon solutions were used with mass loadings of 46 ± 11 μg g^{-1} and 11 ± 1.5 μg g^{-1}. The uncertainties are the standard deviation of three repeated gravimetric determinations. Known amounts of solutions 1 and 2 are mixed with 75 L of artificial seawater to give overall black carbon mass-ratios detailed in table 1. The mass-ratios of black carbon are

Table 1. Optical and physical properties of sea ice for each run including the mass-ratio of black carbon added to the top layer of ice, density of ice and scattering cross-section (σ_{scatt}) of both the top and bottom layers of the ice. The uncertainty in sea ice density is 1 standard deviation of the average of measurements taken from the core profile. Uncertainty is not provided for the density of the top layer as this is the average of only two measurements, although the uncertainty is likely to be similar to that of the lower layer. The mass ratio of black carbon added to the surface layer is also shown. The uncertainty in the black carbon ~~mass ratio~~ mass-ratio is the uncertainty in the gravimetric method used for determining the ~~mass ratio~~mass-ratio, as described on section 2.3.1.

Run number	Black carbon mass-ratio added /ng g^{-1}	Density of bottom (undoped) layer/ g cm^{-3}	Density of top (doped) layer/ g cm^{-3}	σ_{scatt} bottom layer /m^2 kg^{-1}	σ_{scatt} top BC layer /m^2 kg^{-1}
1	0	0.91±0.084	0.92	0.315±0.040	0.05
2	77±18	0.91±0.059	0.91	0.235±0.041	0.05
3	153±37	0.92±0.044	1.00	0.115±0.004	0.35
4	305±62	0.95±0.050	0.93	0.126±0.016	0.2

approximately 0, 75, 150 and 300 ng g^{-1}, these approximate values will be subsequently used in the text whilst precise values are reported in table 1.

2.3.2 Characterisation of black carbon optical properties

The mass absorption cross-section of the black carbon used in the present study is estimated using an integrating sandwich spectrometer, described by Grenfell et al. (2011), based on Clarke (1982). The integrating sandwich spectrometer measures the absorption spectrum of particulate matter on filter samples in a diffuse radiance environment. Absorption spectra of multiple filters containing black carbon loadings are converted to a mass absorption cross-section. ~~Mass absorption cross-sections of 0.58 and~~ A mass absorption cross-section of 2.1 m^{2}g^{-1}, (λ = 610 nm) ~~are~~ is estimated for the black carbon placed in the artificial sea ice. The values are a factor of ~~3–11~~ 3 smaller than the black carbon mass absorption cross-section of 6.57 m^{2}g^{-1}, for a wavelength of 610 nm, (Flanner et al., 2007) typically used in radiative-transfer calculations, but are similar to values used by Dang et al. (2015) owing to the size of the black carbon particles used.

Six known aliquots of the filtered black carbon solution described in section 2.3.1 were filtered through 0.4 μm Nuclepore filters, providing filter loadings of ~~10.076, 15.115, 20.153, 25.191, 50.383 and 100.765~~ 10.18, 15.12, 20.15, 25.19, 50.38 and 100.77 μg cm^{-2}. The absorbance spectra of the filters (figure 4a) is calculated using equation 3:

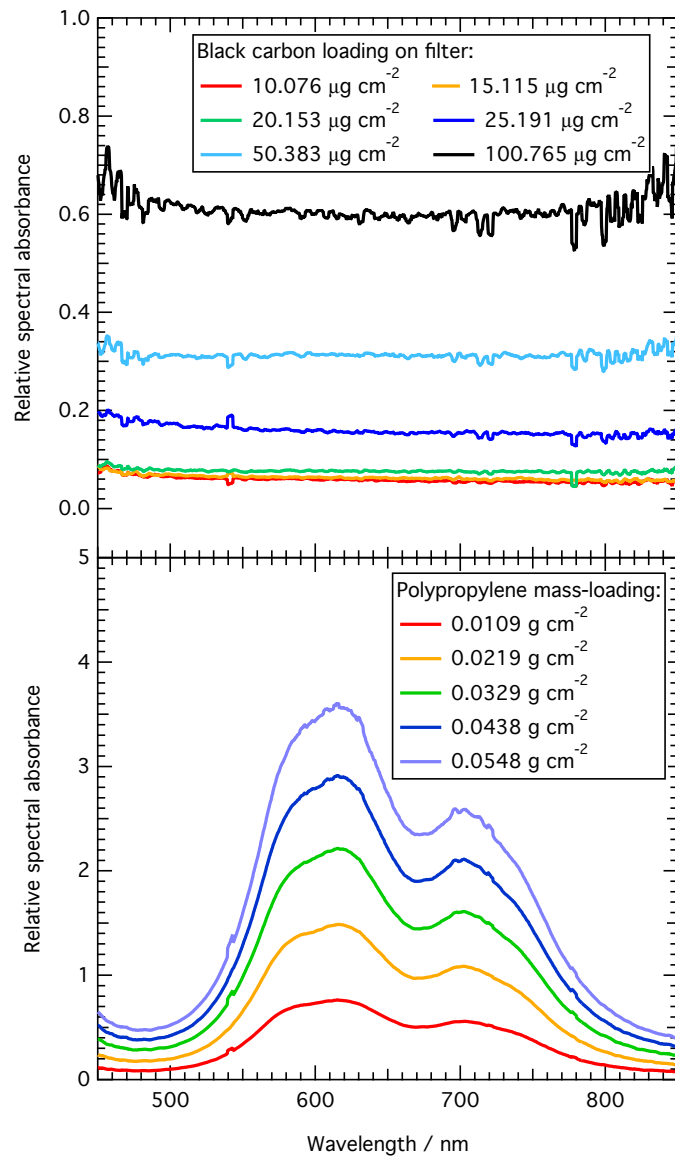$$A(\lambda) = -ln\frac{I(\lambda)}{I_0(\lambda)} \tag{3}$$

Figure 4. ~~Black carbon relative~~ a (top)) Relative spectral absorbance of black carbon versus wavelength for various loadings of black carbon on the filter. b (bottom)~~Acetate calibration sheet relative~~) Relative spectral absorbance versus wavelength for different mass loadings of polypropylene.

Where I is the intensity measured with the loaded filter in the integrating sandwich spectrometer, and I_0 is the intensity measured when a blank 0.4 μm Nuclepore filter, which is measured following the same procedure as the loaded filter. To calibrate the integrating sandwich spectrometer, ~~two sets~~ a set of translucent standard plastic sheets (~~Light Blue Acetate film, 150μm~~

~~and Light Blue Polypropylene,~~ light blue polypropylene, 100 μm) with measurable mass absorption coefficients are used. The sheets are placed on a 0.4 μm Nuclepore filter and measured in the integrating sandwich spectrometer using the same method as the black carbon filters. Multiple sheets of ~~each plastic type~~ the polypropylene are stacked, providing loadings of ~~0.0254, 0.0508, 0.0762 and 0.1016 g cm^{-2} for the Acetate film (figure 4b) and~~ 0.011, 0.0219, 0.0329, 0.0439 and 0.0548 g cm^{-2} ~~for~~

5   ~~the Polypropylene plastic.~~ (figure 4b)

Grenfell et al. (2011) showed that ~~, for small mass loadings, for small changes in absorbance measured by the integrating sandwich spectrometer the mass loading of the filter and the~~ for small amounts of black carbon the mass loading is directly proportional to the absorbance measured by the integrating sandwich ~~are linearly related~~spectrometer. In this study, we considered the linear sensitivity between the black carbon mass loading and the black carbon absorbance with the ratio between

10   black carbon and ~~plastic~~ polypropylene and we equate the ratio of sensitivities to the ratio of the mass absorption cross-section. Therefore, the mass absorption cross-section of the black carbon is expressed in equation 4:

$$\sigma_{BC} = \sigma_{\rho l}\frac{\alpha_{\rho l}}{\beta_{bc}} \tag{4}$$

where $\alpha_{\rho l}$ is the slope of the linear regression between the mass loading of the ~~plastic~~ polypropylene calibration sheets and the relative absorbance of the ~~plastic~~ polypropylene measured in the integrating sandwich spectrometer, β_{bc} is the slope of the

15   linear regression between the mass loading of the black carbon filters and the relative absorbance of the black carbon measured in the integrating sandwich spectrometer and $\sigma_{\rho l}$ is the mass absorption cross-section of the ~~plastic~~polypropylene, given by the Beer-Lambert law.

The mass absorption coefficients of the ~~accetate and~~ polypropylene sheets are measured ~~in~~ with a standard spectrometer using Beer-Lambert law. The measured mass absorption coefficient is ~~45.77±0.04 cm^{2}g^{-1} (λ = 610 nm) for the Acetate~~

20   ~~plastic and~~ 229.23±0.02 cm^{2}g^{-1} (λ = 610 nm)~~for the Polypropylene plastic~~.

To visually investigate the size and shape of the black carbon particles used in the experiment, scanning electron microscopy (SEM) is employed. Approximately 6 mm wide squares of the 0.4 μm filters containing black carbon particles were cut and glued on standard 12.7 mm diameter SEM stubs using double-faced carbon tabs. The samples were gold coated using a Polaron E5100 Series II Cool Sputter Coater for 3 minutes in air, creating a 45 nm thick coating. SEM images were generated on a

25   Hitachi S3000N scanning electron microscope. The images were obtained at a magnification of ~~4000x~~ ×4000 at a working distance of 12.5 mm, with an acceleration energy of 20 kV and a beam current of 85000 nA. Figure 5 shows a SEM image of black carbon particles on a 0.4 μm Nuclepore filter. The SEM images are analysed using the ImageJ image analysis software (Abramoff et al., 2004), to determine the size distribution and the circularity of the black carbon particles. The circularity of the particles is determined by the shape factor Heilbronner and Barrett (2013), ~~caculated~~ calculated using equation 5:

30   $$SF = \frac{4\pi A}{P^2} \tag{5}$$

Where A is the area of the shape and P, the perimeter of the shape. The shape factor represents the deviation of the perimeter of a particle from a circle of the same area. Values of the shape factor vary between 0, representing an elongated shape and

1, describing a circle. The average shape factor of the particles shown in figure 5 is 0.842, indicating a rough spherical shape. Assuming a spherical nature of the particles, the diameter is calculated as the maximum Feret diameter. The average diameter of the particles shown in figure 5 is 0.461 ± 0.331 (2σ) μm.
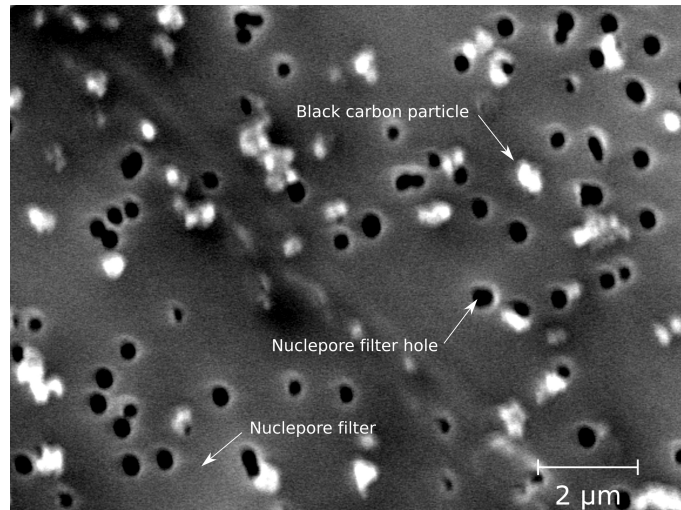

Figure 5. Scanning electron microscope image of gold coated black carbon particles (white) at a magnification of ~~x4000~~$\times$4000, showing a roughly spherical shape of the particles and an average particle diameter of 0.461 ± 0.331 μm. Note the image also shows the Nuclepore filter holes at 0.4 μm diameter

The mass absorption coefficients of the black carbon is also estimated by a Mie light scattering calculation using the SEM
5   data. Mie calculations are performed using size data from the SEM to provide a check of the value for black carbon absorption-cross section for the radiative-transfer calculations. For the Mie calculations the black carbon diameter of 0.461 μm is used with a density of 1.8 g cm^{-3} and a commonly used refractive index of 1.8 – 0.5 ~~Clarke and Noone (1985)~~(Clarke and Noone, 1985), giving an absorption cross section at a wavelength of 550 nm of 2.78 m^{2}g^{-1}.

In the work presented here a absorption cross-section value of 2.5 m^{2}g^{-1} will be used for radiative-transfer calculations, as
10   this is between the values from the Mie calculations and ~~the upper limit of values~~ from the integrating sandwich spectrometer.

3   TUV-snow radiative-transfer calculations

Calculations using the TUV-snow radiative transfer model (described in section 3.1) are undertaken to simulate optical and physical properties measured of the sea ice. For undoped ice reflectance and extinction coefficient/*e*-folding depth are calculated (section 3.2) while for sea ice with black carbon the model is used to calculate only reflectance ~~owing to black carbon~~ (section
15   3.3).

13

3.1 The TUV-snow radiative-transfer model

The TUV-snow model is a coupled atmosphere-snow-sea ice radiative-transfer model using the DISORT code (Stamnes et al., 1988) and is described in detail by Lee-Taylor and Madronich (2002). The model ~~parameterizes~~ parameterises sea ice optical properties using only an asymmetry factor, g, a wavelength independent scattering cross-section, σ_{scatt}, a wavelength dependant absorption cross-section, σ_{abs}^{+}, and sea ice density and thickness.

3.2 Calculations of undoped ice reflectance and extinction coefficient/e-folding depth

The reflectance and extinction coefficient/e-folding depth of the undoped sea ice are calculated through radiative-transfer calculations using the TUV-snow model with derived scattering and absorption cross sections for the ice. To derive these values, values of scattering and absorption cross section are varied until they reproduce the experimentally measured reflectivity and e-folding depth data for the sea ice as detailed in King et al. (2005); France et al. (2011, 2012); Marks and King (2014). Ice density and thickness are measured from ice cored at the end of an experiment. The density of the ice is detailed in table 1. The ice is modelled with a 30 cm thick bottom layer subdivided into 45 sub-layers with each sub-layer representing 1 cm apart from the bottom and top 5 sub-layers which are ~~1mm~~ 1 mm thick. The asymmetry factor for the ice is fixed at 0.95, based on a value suggested by Mobley et al. (1998) for a bubble rich ice, which is observed in ice cores taken from the tank.

All calculations are undertaken between wavelengths 350–650 nm, using eight-streams in DISORT. The ~~reflectance under the ice is the measured, wavelength dependent~~ wavelength dependant, nadir reflectance of the ~~bottom of the~~ water filled tank is measured and included in the model as the under ice reflectance, the measurements are included in the supplementary information. The model illuminates the ice with diffuse light.

Reflectivity is calculated as the ratio of upwelling, Irr_{up}, to downwelling Irr_{down}, irradiance at the surface of the sea ice, $\left(\frac{Irr_{up}}{Irr_{down}}\right)$. The e-folding depth is calculated using equation 2, and the irradiances calculated at depths of 5, 10, 15 and 20 cm in the sea ice with reference irradiance at a depth of 5 cm (to reproduce experimentally derived e-folding depths). The extinction coefficient is calculated as the reciprocal of the value of e-folding depth.

3.3 Calculating surface reflectance of ice with a black carbon doped layer

The radiative transfer modelling was repeated for the black carbon doped sea ices. For these radiative transfer calculations parameters are kept the same as the undoped ice calculations, although the ice is modelled as two layers; a 30 cm thick undoped bottom layer and a 5 cm upper, black carbon bearing, layer. These principal layers are subdivided into 45 sub-layers for the bottom layer and 14 sub-layers in the top layer, with each sub-layer being 1 cm thick, apart from 0.5 cm either side of a boundary (air-ice, undoped ice-doped ice and ice-water), where sub-layers are 1 mm.

The absorption cross-section of the top layer was the same as the bottom undoped layer plus additional absorption for any black carbon present (0, 75, 150 and 300 ng g^{-1}), where the absorption cross-section of the black carbon is 2.5 m^{2}g^{-1} (see section 2.3.2). The scattering cross-section of the top layer was derived by a trial and error method to obtain the best fit (judged

by eye) between modelled and measured values of reflectance and *e*-folding depth as described in section 4.3. Densities of the top layers are shown in table 1.

4 Results

4.1 Physical properties of sea ice and growth rates

5 Salinity, density and temperature depth profiles of all ice cores are given in the supplementary information. A typical salinity and temperature profile is given in figure 6. The average density for the top and bottom layer for each black carbon loading is shown in table 1.
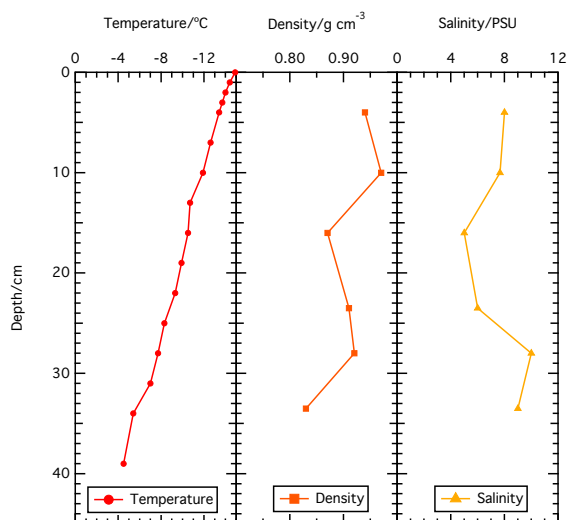

Figure 6. Example temperature, salinity and density data for an ice core from run 2 before the black carbon bearing layer was added.

Ice growth rates were similar for all runs with the ice growing at approximately 1.8 cm per day. For all runs the growth rate gradually declined as ice growth progressed. The time taken for reflectance of the ice to become a constant value became 10 longer, taking 5 days for run 1, 7 days for run 2, 11 days for run 3 and 13 days for run 4 owing to an issue with the maintenance of the refrigerator plant which reduced its heat flux but not its maintained temperature. The sea ice produced for each run had a slightly different fabric and subsequently produced less scattering sea ice as shown by the value of σ_{scatt} in table 1.

4.2 Measured and modelled reflectivity and ~~e-folding~~ extinction coefficient/*e*-folding depth of undoped sea ice

4.2.1 Experimental measurements and calculations of reflectance and ~~e-folding~~ extinction coefficient/*e*-folding depth for undoped ice

The measured nadir reflectance of the undoped ice layer, is shown in figure 7 for the four runs. Each run represents an experiment with new sea ice growth before the black carbon bearing layer is added. The reflectance is wavelength dependent peaking at values around 500 nm, as would be expected for sea ice (e.g. Grenfell and Maykut (1977)). Measurements of reflectance shown in figure 7 are the average of 5 days of reflectance measurements taken when ice reflectance had become constant. The reflectance of the undoped sea ice decreases from run 1 to run 4 which is attributable to the slightly different ice fabrics in each run and the fact that the ice thickness is not optically thick.
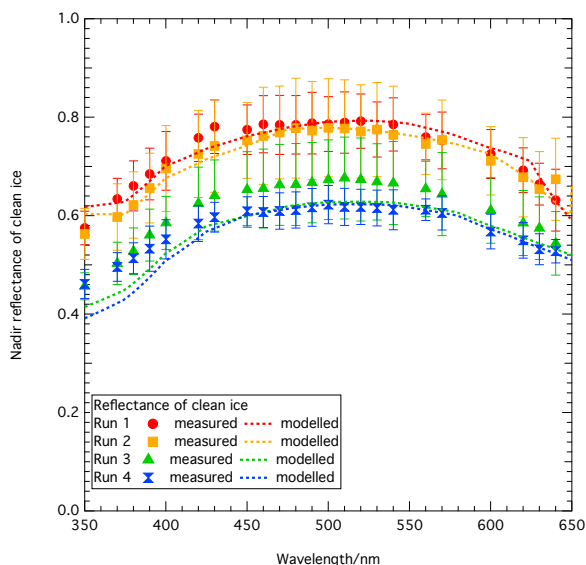

Figure 7. Measured sea ice surface reflectance versus wavelength (solid shapes) and modelled sea ice reflectance versus wavelength (dashed lines) for sea ice with no added black carbon

The extinction coefficient and *e*-folding depth of the undoped ice, figure 8, ~~is~~ are also wavelength dependent with the largest values of *e*-folding depth observed around 550 nm for all runs again representing a natural sea ice (e.g. Grenfell and Maykut (1977)). The *e*-folding depths increase with run number which is again attributable to the different ice fabrics created. The increased *e*-folding depth can be attributed to a less light scattering sea ice matrix.

Figures 7 and 8 also contain the modelled reflectivity and extinction coefficient/*e*-folding depth fitted to the experimental data. With the exception of the UV nadir reflectivity of run 3 and 4 the modelled fits are well within uncertainty of the measurement.

It should be noted it is more difficult to find a pair of values for scattering and absorption cross-sections (σ_{scatt} and σ_{abs}^+) for each wavelength that produce a good reproduction of the experimental reflectivity *and e*-folding depth, rather than reflectivity alone, as the system described here is significantly more constrained in the number of degrees of freedom. Thus measuring reflectivity and *e*-folding depth gives the reader more confidence in the values of σ_{scatt} and σ_{abs}^+.
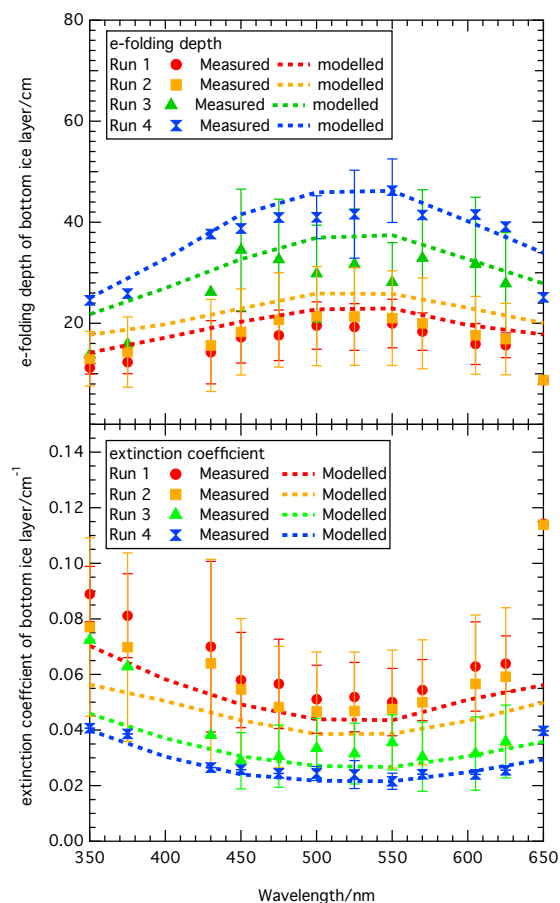

Figure 8. a (top)) Measured sea ice *e*-folding depth versus wavelength (solid shapes) and modelled sea ice *e*-folding depth versus wavelength (dashed lines) for sea ice with no added black carbon. b (bottom)) Measured sea ice extinction coefficient versus wavelength (solid shapes) and modelled sea ice extinction coefficient versus wavelength (dashed lines).

5   **4.2.2   Derived absorption and scattering cross-sections from experimental data for undoped ice**

The calculated values of the absorption cross-section of impurities in the undoped ice used in the radiative transfer calculations are shown in figure 9. Ideally this absorption should be zero for undoped ice (no impurities) but a characteristic signal of algae

17

is present (e.g. Bricaud et al. (2004)). The shape of the derived absorption cross-section for each run is similar, decreasing slightly with increased run number.

It should be noted that the algae was unintentional, not observed by the naked eye and resisted several cycles of disinfection. It is testament to the sensitivity of the technique for deriving absorption and scattering cross-sections that the absorption cross-section of the algae can be calculated.
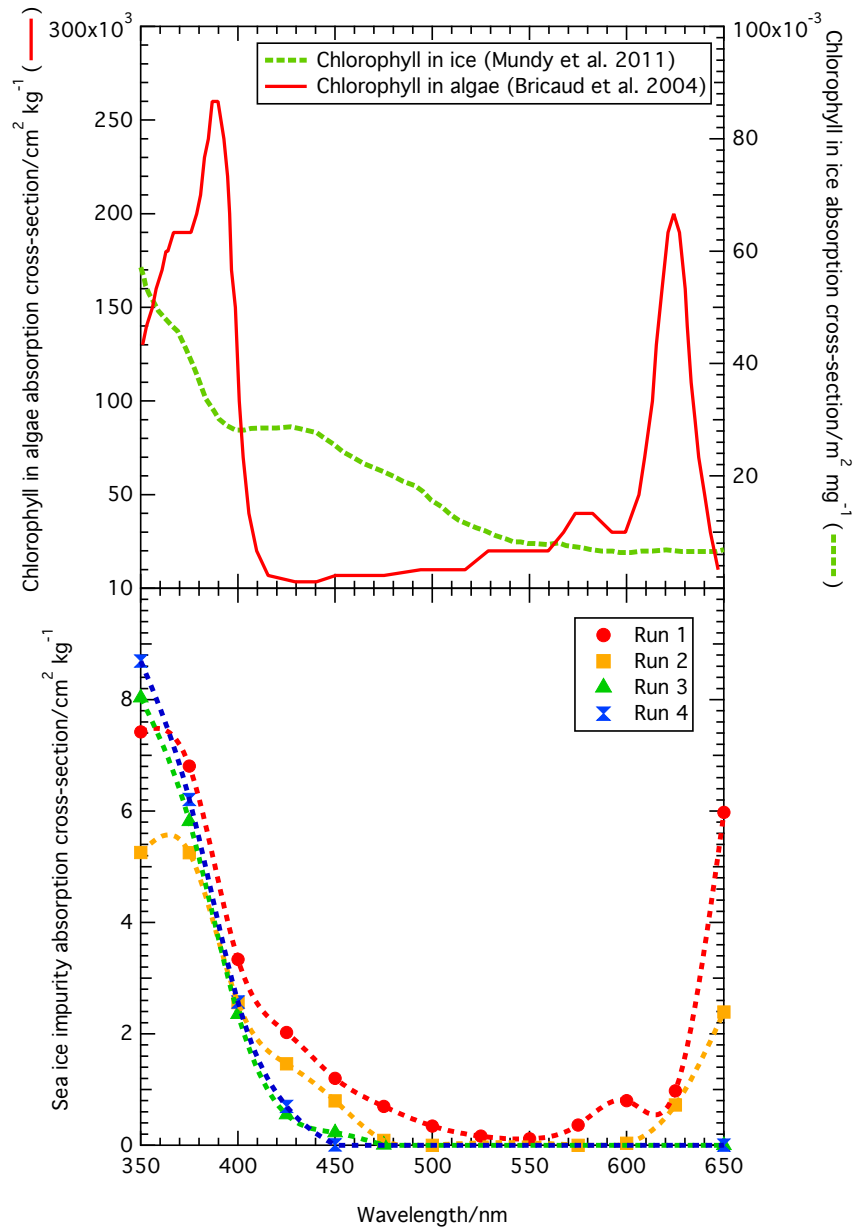
Figure 9. a (top)) Absorption cross-sections of chlorophyll. Chlorophyll in ice (dashed line) taken from Mundy et al. (2011) is per mg of algae determined by fluorescence. Chlorophyll (solid line) is taken from Bricaud et al. (2004) is per mg of dry weight cells. b (bottom)) Wavelength dependent absorption cross-section derived from reflectance and *e*-folding depth data from runs 1 to 4 for the undoped ice. A smooth line is added to guide the eye. Values for run 4 are too small to plot clearly at longer wavelengths. Error bars show the possible variation in absorption cross-section obtained from different fits of the original reflectance and *e*-folding depth data.

The modelled scattering coefficient used in the radiative-transfer calculations is wavelength independent and reported in table 1.

4.3 Surface reflectivity of black carbon doped sea ice

The reflectance of the sea ice with an extra 5 cm black carbon bearing ice layer decreases at all wavelengths as the black carbon mass-ratio increases; as shown in figure 10. At a wavelength of 500 nm, reflectance decreases to 97% of the reflectance of undoped ice (Run 1) for an addition of seawater with a mass ratio of black carbon of 75 ng g^{-1}, to 90% for an addition with a mass-ratio of 150 ng g^{-1} compared to undoped ice and to 79% for an addition with a mass ratio of 300 ng g^{-1} compared to reflectivity of undoped ice.
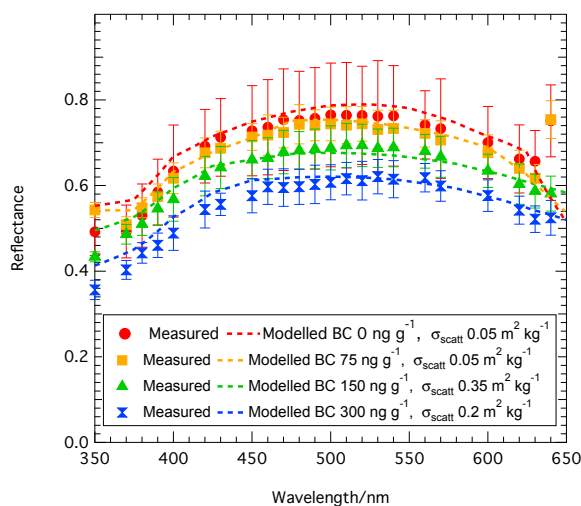

Figure 10. Comparison between measured (solid shapes) and calculated (dashed lines) reflectance of ~~simulated~~ laboratory sea ice surface with black carbon in a 5 cm surface layer in varying mass ratios. The figure shows the best fit possible by altering scattering cross-section of the upper black carbon bearing layer (values shown on plot).

The extinction coefficient/e-folding depth of the ice after the black carbon layer was added was not measured as the total ice could no longer be considered a homogeneous medium and the 5 cm doped layer was too thin to measure the ~~folding depth for~~ extinction coefficient in this layer alone.

The best fit obtained between the measured and calculated reflectance values from varying the scattering cross-section of the upper sea ice layer between realistic values is shown in figure 10. These values of the scattering cross-section are shown in figure 10, varying from 0.05 m^2 kg^{-1} to 0.35 m^2 kg^{-1}. The fit between the measured and calculated reflectance is well within uncertainty limits for all runs demonstrating the TUV-snow model can reproduce experimental ~~albedos~~ reflectance for sea ice doped with black carbon, even with varying fabrics of sea ice.

5 Discussion

In the discussion section possible sources of uncertainty in the experimental measurements compared to the calculated values will be discussed as well as the realism of the ~~simulated~~ laboratory sea ice and potential limitations of the sea ice simulator.

5.1 Sources of uncertainty in the experimental measurements compared to the calculated values

5   The comparison between experimentally measured and calculated values reported here are presented under the assumption that the experimental conditions are accurately replicated by the TUV-snow radiative-transfer model. Potential sources for uncertainty in comparing experimentally measured values to calculated values include: aggregation of black carbon particles; mobilisation of black carbon from the top layer of sea ice into the underlying ice and sea water; the value of the asymmetry parameter used in the radiative transfer modelling; uncertainty in the derived scattering and absorption cross-sections of the

10   experimental sea ice and uncertainty in the mass ratio of black carbon added to the ~~simulated~~ laboratory sea ice. The possible contribution of each of these factors is subsequently reviewed.

5.1.1 Aggregation of particles

The effect of aggregation of black carbon particles decreases the absorption cross-section in two ways. Assuming two black carbon particles aggregate to form a new spherical black carbon particle, the newly formed particle would have twice the

15   volume and the radius would be a factor of $\sqrt[3]{2}$ larger. Mie calculations show that the absorption cross-section would decrease and the mass-absorption cross-section would decrease and flatten according to Dang et al. (2015). Secondly aggregation would reduce the number density of black carbon particles further reducing the absorption of light within the ice. However, the good agreement shown between measured and calculated reflectance for the black carbon doped ice suggests aggregation is not occurring within the ice.

5.1.2 Black carbon mobilisation

The radiative-transfer model assumes the black carbon is distributed evenly within the black carbon doped layer, however the experimental ice may not have had an even distribution. Sea ice ~~is at its eutectic point and~~ forms brine pockets and brine channels on freezing (e.g. Weeks (2010)). As the extra layer of seawater freezes brine will drain downwards into the layer of ice below and also be expelled onto the surface. Eicken (2003) suggest that impurities in seawater are trapped in the brine

25   inclusions as sea ice grows. If black carbon is situated in brine inclusions then some of it may drain into the underlying layer of sea ice and eventually into the underlying seawater as described by Eicken (2003). Doherty et al. (2010), who measured black carbon mass-ratios in sea ice in the Arctic, showed that black carbon is concentrated at the surface of the sea ice but also found in smaller concentrations throughout the ice, supporting the idea that black carbon deposited onto the surface of sea ice can be mobilised through the ice. If there was a reduced black carbon mass ratio in the upper layer then surface reflectance would

30   increase (e.g. Marks and King (2013)).

5.1.3 Asymmetry parameter

A value of the asymmetry parameter, ~~g~~g, of 0.95 was used based on the work of Mobley et al. (1998). However Mobley et al. (1998) demonstrate that g may vary between 0.94 and 0.99. Figure 11 shows the effect on the determination of the absorption cross-section, σ_{abs} owing to absorption by impurities and the ice scattering cross-section at 400 nm for changing the value of g within possible values for sea ice; 0.94–0.99 (Mobley et al., 1998).
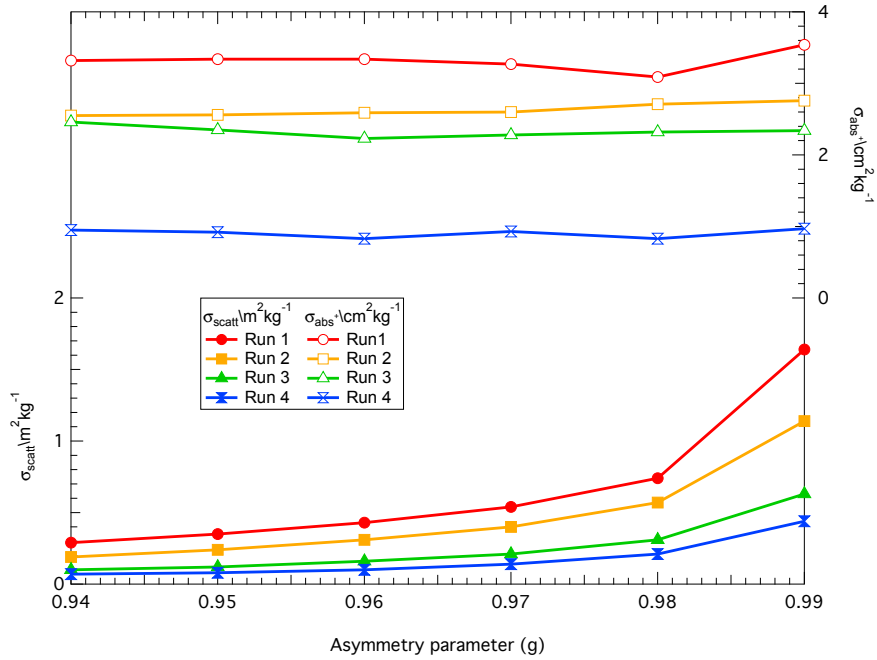

Figure 11. Variation in absorption cross-section, σ_{abs}^{+}, (cm^2 kg^{-1}) (~~dashed line~~upper, non-filled markers) and scattering cross-section, σ_{scatt}, (m^2 kg^{-1}) (~~solid line~~lower, filled symbols) owing to variation in the asymmetry parameter at 400 nm. Note the scatter in the values of σ_{abs}^{+} is due to the fitting process used.

The change in the g value has very little effect on the values of absorption cross-section, as also noted by Libois et al. (2013), with ~~the standard deviation of σ_{abs}^{+} across g =~~ variation in g between 0.94 ~~–0.99~~ to 0.99 having only a factor of 0.092 effect on the absorption cross-section, demonstrating the model is insensitive to the value of g for determining light absorbing impurities.

In the case of scattering cross-section, the effect of changing g from 0.94 ~~–0.99~~ to 0.99 at 400 nm has a much larger effect on the scattering cross-section, with a larger g value giving a larger scattering cross-section ~~–~~i.e. the similarity principle. An increase in the scattering cross-section would change the shape of the reflectance-wavelength curve as well as the values of reflectance, as absorbing impurities have less effect in a sea ice with a large scattering cross-section compared to a small one, as described in Marks and King (2014).

5.1.4 Uncertainty in derived scattering and absorption cross-section and black carbon mass ratio

~~There is a small degree of uncertainty in deriving the~~

The determination of the cross-section for light scattering and absorption, described in section 4.2.2, depends on varying their values to reproduce the measured values of the e-folding depth and the nadir reflectivity within the experimental uncertainties of measured values of the e-folding depth and the nadir reflectivity, all as a function of wavelength. The latter assists in constraining the determination of the values of the cross-section for absorption and scattering. The propagated uncertainty in the determined values of the cross-sections for light scattering and absorption ~~cross-section by modelling from~~ from uncertainties in either the value of the e-folding depth or nadir reflectivity in isolation have not been calculated as our method fits both e-folding depth and reflectivity. Considering the experimental uncertainty in e-folding depth and nadir reflectivity gives a more representative uncertainty of the process. The uncertainty in the reflectance and e-folding depth measurement data of the undoped ice ~~shown in figure 9 and table 1. The uncertainty was~~ is shown in figures 7 and 8. Table 1 gives an indication of the uncertainty in the derived scattering cross-section which is estimated by varying the values of σ_{scatt} and σ_{abs} and still obtaining a good fit (by eye) to the experimental data within the uncertainties of the measured e-folding depth and nadir reflectivity.

5.2 Realism of artificial sea ice

The sea ice simulator is designed to replicate natural sea ice growth in a controlled environment. Section 5.2 will review how the measured physical and optical parameters of the sea ice compare to field measurements of sea ice to ascertain how the ~~simulated~~ laboratory sea ice compares to natural ice. Although the simulator creates a realistic sea ice environment, as with all simulators, there are limitations in the degree to which a "natural" sea ice environment can be created~~, limitations~~. Limitations in the following metrics were noted; light intensity, uneven ice growth, hyper-saline seawater, surface brine expulsion and reflectance measurements.

5.2.1 Physical properties

Temperature profiles from the ~~simulated~~ laboratory sea ice show a linear increase in temperature from the surface to the ice base, this has been commonly reported (e.g. Eicken (2003); Perovich et al. (1998b)). Eicken (2003) also suggest that at typical winter temperatures ice would take ~1 month to form 50 cm, this is a similar growth rate to that observed for the laboratory grown sea ice where it took approximately three weeks to grow 30 cm of ice.

Typical sea ice densities are reviewed by Timco and Frederking (1996) reporting first year sea ice densities in the range 0.84 to 0.94 g cm^{-3}, the density of sea ice created in the simulator ranged from 0.85 to 0.95 g cm^{-3}, thus being in the range of natural ice. Perovich et al. (1998b) measured density profiles through Arctic first year sea ice showing no clear variation with depth which is also observed in the ~~simulated~~ laboratory sea ice.

Plots of salinity versus depth from ice cores from the sea ice simulator show the distinctive "C" shape with a higher salinity seen at the base and top of the cores, see figure 6. Malgrem et al. (1927) studied salinity of first-year ice also showing a characteristic "C" shape to the sea ice salinity profile. The shape of the salinity profile, explained by Eicken (2003), is due

to a combination of salt segregation, gravity drainage and brine expulsion on the surface of the ice. Initially as sea ice in the simulator grows the seawater below the ice increases in salinity and similarly to natural sea ice the seawater below the ice is commonly hyper-saline. As the simulator continues to generate thicker sea ice there is an increase in the salinity of the brine beneath the sea ice which may eventually retard the growth and the water may become unrealistically saline if the experiment were allowed to continue. In the experiment discussed here this is not a major problem for the experiments as the experiments were performed with ice thicknesses of 30 cm.

The typical structure of a first year sea ice is described by Eicken (2003) showing a granular surface layer, overlying columnar ice with granular/platelet ice at the ice-water boundary. The structure described by Eicken (2003) is the same as that observed in ice cores of the laboratory grown ice. The surface of the laboratory grown ice has a clear granular texture, and at the base there is a slushy platelet layer with columnar ice in between.

Although the sides of the tank are insulated ice growth across the tank is not quite uniform with slightly thicker ice (∼5 cm) around the edges of the tank towards the end of an experiment (∼3 cm from the sides) and around the polypropylene pole which the thermocouples were inserted into. Unfortunately the thicker ice areas could not be rectified but are unimportant as reflectance measurements were taken in the same place, away from the sides of the tank.

5.2.1 ~~Optical properties~~

~~The reflectance of various Arctic sea ice types are reported by Grenfell and Maykut (1977). Figure ?? shows a comparison of the average optically thick reflectance of the laboratory grown sea ice in comparison to the reflectance reported by Grenfell and Maykut (197 The reflectance of the laboratory gown ice is considerably larger than a first year ice resembling a reflectance closer to a multi-year ice. The difference may be due to the reflecting surface under the laboratory sea ice being a tank as opposed to a comparatively unreflective ocean. In the radiative-transfer calculations described here the shallow depth of the sea ice tank is accounted for by measurement of its reflectivity.~~

~~Comparison of measured sea ice simulator ice reflectance (red dots) to reflectance values of sea ice measured in the field by Grenfell and Maykut (1977) (black lines).~~

~~Typical~~ All measurements of the extinction coefficient/*e*-folding ~~depths~~ depth were made more than three *e*-folding depths from the sides of the tank so that any extra ice growth at the edges of the tank would have no impact on the measurements. Typical extinction coefficients of sea ice at around 500 nm ~~range from~~ are around ∼~~1 m for a first year blue ice to ∼35 cm for a multi-year granular white ice~~ 0.03 cm^{-1} (Grenfell and Maykut, 1977). Calculated ~~-folding depths~~ extinction coefficients for the laboratory grown ice range from ~~10–35 cm. The shorter -folding depths calculated for the laboratory grown ice is likely to be due to light reflected from the bottom of the tank and is accounted for in the radiative-transfer modelling.~~ 0.1–0.03 cm^{-1}.

Overall the sea ice simulator creates a realistic sea ice, recreating typical growth rates, salinity and temperature profiles, reflectance and ~~-folding depths~~ extinction coefficients of a first year sea ice.

6 Conclusions

The study has shown that the TUV-snow radiative transfer model can reproduce ~~albedo~~ reflectivity of undoped and black carbon doped sea ice with different sea ice fabrics and thus the model can be used with confidence. Black carbon in ~~simulated~~ laboratory sea ice has been shown to reduce the ~~albedo~~ reflectivity of the ice ~~by~~ to 97%, 90%, and 79% ~~compared to clean ice~~ of the clean ice reflectivity at a wavelength of 500 nm for mass ratios of 75, 150 and 300 ng g^{-1} of black carbon respectively in the top 5 cm layer of the ~~simulated~~ laboratory sea ice, which is in agreement with radiative-transfer calculations. To reproduce the ~~albedo using the the~~ reflectivity using the TUV-snow model measured ~~albedo~~ reflectivity and *e*-folding depth data from ~~simulated~~ laboratory sea ice is used to derive scattering and absorption cross-sections of the ice using the TUV-snow model. The derived scattering cross-section values are typical of sea ice (e.g. Grenfell and Maykut (1977), Timco and Frederking (1996) and Perovich (1996), while the derived absorption cross-sections show the presence of other absorbing impurities in the undoped ice, which matches the absorption spectra of algae.

References

Abramoff, M., Magalhaes, P., and Ram, S.: Image Processing with ImageJ, Biophotonics International, 11, 36–42, 2004.

Atkinson, M. and Bingman, C.: Elemental composition of commercial seasalts, Journal of Aquariculture and Aquatic Sciences, 8, 39, 1997.

Ball, C., Levick, A., Woolliams, E., Green, P., Dury, M., Winkler, R., Deadman, A., Fox, N., and King, M.: Effect of polytetrafluoroethylene (PTFE) phase transition at 19 °C on the use of Spectralon as a reference standard for reflectance, Applied Optics, 52, 4806–4812, 2013.

Bond, T., Doherty, S., Fahey, D., Forster, P., Berntsen, T., DeAngelo, B., Flanner, M., Ghan, S., Kärcher, B., and Koch, D.: Bounding the role of black carbon in the climate system: A scientific assessment, Journal of Geophysical Research: Atmospheres, 118, 5380–5552, 2013.

Boyer, T., Antonov, J., Baranova, O., Coleman, C., Garcia, H., Grodsky, A., Johnson, D., Locarnini, R., Mishonov, A., O'Brien, T., Paver, C., Reagan, J., Seidov, D., Smolyar, I., and Zweng, M.: World Ocean Database 2013, Tech. Rep. NOAA Atlas NESDIS 72, National Oceanic and Atmospheric Administration, 2013.

Brandt, R. E., Warren, S. G., and Clarke, A. D.: A controlled snowmaking experiment testing the relation between black carbon content and reduction of snow albedo, Journal of Geophysical Research: Atmospheres, 116, 2011.

Bricaud, A., Claustre, H., Ras, J., and Oubelkheir, K.: Natural variability of phytoplanktonic absorption in oceanic waters: Influence of the size structure of algal populations, Journal of Geophysical Research, 109, 2004.

Buist, I., Potter, S., Nedwed, T., and Mullin, J.: Herding surfactants to contract and thicken oil spills in pack ice for in situ burning, Cold regions science and technology, 2011.

Clarke, A.: Integrating sandwich: a new method of measurement of the light absorption coefficient for atmospheric particles, Applied Optics, 21, 1982.

Clarke, A. and Noone, K.: Soot in the Arctic snowpack: A cause for perturbations in radiative transfer, Atmospheric Environment (1967), 19, 2045–2053, 1985.

Dang, C., Brandt, R. E., and Warren, S. G.: Parameterizations for narrowband and broadband albedo of pure snow and snow containing mineral dust and black carbon., Journal of Geophysical Research: Atmospheres, 120, 5446–5468, 2015.

Doherty, S., Warren, S., Grenfell, T., Clarke, A., and Brandt, R.: Light-absorbing impurities in Arctic snow, Atmospheric Chemistry and Physics, 10, 18 807–18 878, 2010.

Eicken, H.: Sea ice-an introduction to its physics, biology, chemistry and geology, chap. From the microscopic, to the macroscopic, to the regional scale: growth, microstructure and properties of sea ice, Blackwell Science, London, 2003.

Flanner, M., Zender, C., Randerson, J., and Rasch, P.: Present-day climate forcing and response from black carbon in snow, Journal of Geophysical Research, 112, 2007.

France, J. and King, M.: The effect of measurement geometry on recording solar radiation attenuation in snowpack (e-folding depth) using fibre-optic probes, Journal of Glaciology, 58, 2012.

France, J., King, M., Frey, M., Erbland, J., Picard, G., Preunkert, S., MacArthur, A., and Savarino, J.: Snow optical properties at Dome C (Concordia), Antarctica; implications for snow emissions and snow chemistry of reactive nitrogen, Atmospheric Chemistry and Physics, 11, 9787–9801, 2011.

France, J., Reay, H., King, M., Voison, D., Jacobi, H., Domine, F., Beine, H., Anastasio, C., MacArthur, A., and Lee-Taylor, J.: Hydroxyl Radical and NO_x producion rates, black carbon concentrations and light-absorbing impurities in the snow from field measurements of light penetration and nadir reflectivity of on-shore and off-shore coastal Alaskan snow, Journal of Geophysical Research, 117, 2012.

Goldenson, N., Doherty, S., Bitz, C., and Holland, M.: Arctic climate response to forcing from light-absorbing particles in snow and sea ice in CESM, Atmospheric Chemistry and Physics, 12, 7903–7920, 2012.

Grenfell, T. and Maykut, G.: The optical properties of ice and snow in the Arctic Basin, Journal of Glaciology, 18, 1977.

Grenfell, T. and Perovich, D.: Radiation absorption coefficients of polycrystalline ice from 400–1400 nm, Journal of Geophysical Research, 86, 7447–7450, 1981.

Grenfell, T., Light, B., and Sturm, M.: Spatial distribution and radiative effects of soot in the snow and sea ice during the SHEBA experiment: The surface heat budget of Arctic ocen (SHEBA), Journal of Geophysical Research, 107, 2002.

Grenfell, T., Doherty, S., Clarke, A., and Warren, S.: Light absorption from particulate impurities in snow and ice determined by spectrophotometric analysis of filters, Applied Optics, 50, 2037–2048, 2011.

Haas, C., Cottier, F., Smedsrud, L., and Thomas, D.: Multidisciplinary ice tank study shedding new light on sea ice growth processes, EOS, Transactions, 80, 507–513, 1999.

Hadley, O. and Kirchstetter, T.: Black carbon reduction of snow albedo, Nature Climate Change, 2, 437–440, 2012.

Hansen, J. and Nazarenko, L.: Soot climate forcing via snow and ice albedos, Proceedings of the National Academy of Sciences of the United States of America, 101, 423, 2004.

Hare, A., Wang, F., Barber, D., Geilfus, N., and Galley, R.: pH evolution in sea ice grown at an outdoor experimental facility, Marine Chemistry, 2013.

Heilbronner, R. and Barrett, S.: Image analysis in Earth Sciences: microstructures and textures of earth materials, Springer Science and Business Media, 129, 2013.

Highwood, E. and Kinnersley, R.: When smoke gets in our eyes: The multiple impacts of atmospheric black carbon on climate, air quality and health, Environment international, 32, 560–566, 2006.

Holland, M., Bailey, D., Breigleb, B., Light, B., and Hunke, E.: Improved sea ice short wave radiation physics in CCSM4: The impact of melt ponds and aerosols on Arctic sea ice, Journal of Climate, 25, 1413–1430, 2012.

IPCC: IPCC Working Group 1 Fifth Assessment Report Summary for Policy Makers - Climate Change 2013: The Physical Science Basis., Tech. rep., IPCC, 2013.

Jacobson, M.: Strong radiative heating due to the mixing state of black carbon in atmospheric aerosols, Nature, 409, 695–697, 2001.

Jacobson, M.: Climate response of fossil fuel and biofuel soot, accounting for soot's feedback to snow and sea ice albedo and emissivity, Journal of Geophysical Research, 109, 2004.

Johnston, M. and Timco, G.: Temperature Changes in First Year Arctic Sea Ice During the Decay Process., in: Proceedings of the 16th IAHR International Symposium on Ice, vol. 2, pp. 194–202, 2002.

King, M., France, J., Fisher, F., and Beine, H.: Measurement and modelling of UV radiation penetration and photolysis rates of nitrate and hydrogen peroxide in Antarctic sea ice: An estimate of the production rate of hydroxyl radicals in first-year sea ice, Journal of Photochemistry and Photobiology A: Chemistry, 176, 39–49, 2005.

Krembs, C., Mock, T., and Gradinger, R.: A mesocosm study of physical-biological interactions in artificial sea ice: effects of brine channel surface evolution and brine movement on algal biomass, Polar Biology, 24, 356–364, 2001.

Lamare, M. L., Lee-Taylor, J., and King, M. D.: The impact of atmospheric mineral aerosol deposition on the albedo of snow and sea ice-are snow and sea ice optical properties more important than mineral aerosol optical properties?, Atmospheric Chemistry and Physics, 16, 843–860, 2016.

Ledley, T. and Thompson, S.: Potential effect of nuclear war smokefall on sea ice, Climatic Change, 8, 155–171, 1986.

Lee-Taylor, J. and Madronich, S.: Calculation of actinic fluxes with a coupled atmosphere-snow radiative transfer model, Journal of Geophysical Research, 107, 2002.

Libois, Q., Picard, G., France, J., Arnaud, L., Dumont, M., Carmagnola, C., and King, M. D.: Influence of grain shape on light penetration in snow, The Cryosphere, 7, 1803–1818, 2013.

5 Light, B., Eicken, H., Maykut, G., and Grenfell, T.: The effect of included particulates on the spectral albedo of sea ice, Journal of Geophysical Research, 103, 27 739–27 752, 1998.

Light, B., Carns, R., and Warren, S.: "Albedo dome": A method for measuring spectral flux-reflectance in a laboratory for media with long optical paths, Applied Optics, 54, 2015.

Malgrem, F., Institutt, G., Forskningsfond, S., and Fond, N.: The Norwegian Polar Expedition 'Maud,' 1918–1925:Scientific Results, vol. 1,
10 chap. On the properties of sea-ice, pp. 1–67, Gofys. Inst., Bergen, Norway, 1927.

Marks, A. and King, M.: The effects of additional black carbon on the albedo of Arctic sea ice: variation with sea ice type and snow cover, The Cryosphere, 7, 1193–1204, 2013.

Marks, A. and King, M.: The effect of snow/sea ice type on the response of albedo and light penetration depth (e-folding depth) to increasing black carbon, The Cryosphere, 8, 1023–1056, 2014.

15 Mitchell, J.: Visual range in the polar regions with particular reference to the Alaskan Arctic, Journal of Atmospheric and Terrestrial Physics Special Supplement, pp. 195–211, 1957.

Mobley, C., Cota, G., Grenfell, T., Maffione, R., Pegau, W., and Perovich, D.: Modeling light propagation in sea ice, Geoscience and Remote Sensing, IEEE Transactions on, 36, 1743–1749, 1998.

Mock, T., Dieckmann, G., Haas, C., Krell, A., Tison, J., Belem, A., Papadimitriou, S., and Thomas, D.: Micro-optodes in sea ice: a new
20 approach to investigate oxygen dynamics during sea ice formation, Aquatic Microbial Ecology, 2002.

Mundy, C., Gosselin, M., Ehn, J., Belzile, C., Poulin, M., Alou, E., Roy, S., Hop, H., Lessard, S., Papakyriakau, T., Barber, D., and Stewart, J.: Characteristics of two distinct high-light acclimated algal communities during advanced stages of sea ice melt, Polar Biology, 34, 1869–1886, 2011.

Nomurai, D., Yoshikawa-Inoue, H., and Toyota, T.: The effect of sea-ice growth on air–sea CO_2 flux in a tank experiment, Tellus B, 58, 2006.

25 Papadimitriou, S., Kennedy, H., Kattner, G., Dieckmann, G., and Thomas, D.: Experimental evidence for carbonate precipitation and CO_2 degassing during sea ice formation, Geochemica et Cosmochimica Acta, 68, 1749–1761, 2003.

Peltoniemi, J., Gritsevich, M., Hakala, T., Dagsson-Waldhauserová, P., Arnalds, Ó., Anttila, K., Hannula, H., Kivekäs, N., Lihavainen, H., Meinander, O., Svensson, J., Virkkula, A., and De Leeuw, G.: Soot on Snow experiment: bidirectional reflectance factor measurements of contaminated snow, The Cryosphere, 9, 2323–2337, 2015.

30 Perovich, D.: The Optical Properties of Sea Ice., US Army Corps of Engineers: Cold Regions Research and Engineering Laboratory, 96, 1996.

Perovich, D. and Grenfell, T.: Laboratory studies of the optical properties of young sea ice, Journal of Glaciology, 27, 1981.

Perovich, D., Roesler, C., and Pegau, W.: Variability in Arctic sea ice optical properties, Journal of Geophysical Research, 103, 1193–1208, 1998b.

35 Phillips, G. and Simpson, W.: Verification of snowpack radiation transfer models using actinometry, Journal of Geophysical Research, 110, 2005.

Polach, R., Ehlers, S., and Kujala, P.: Model-Scale Ice-Part A: Experiments, Cold regions science and technology, 94, 74–81, 2013.

Rabus, B. and Echelmeyer, K.: Increase of 10 m ice temperature: climate warming or glacier thinning?, Journal of Glaciology, 48, 2002.

Ramanathan, V. and Carmichael, G.: Global and regional climate changes due to black carbon, Nature Geoscience, 1, 221–227, 2008.

Rand, J. and Mellor, M.: Ice-coring augers for shallow depth sampling, Tech. Rep. 85-21, CRREL, Washington, 1985.

Reay, H., France, J., and King, M.: Decreased albedo, efolding depth and photolytic OH radical and NO_2 production with increasing black carbon content in Arctic snow., Journal of Geophysical Research, 117, 2012.

5 Stamnes, K., Tsay, S., Jayaweera, K., and Wiscombe, W.: Numerically stable algorithm for discrete-ordinate-method radiative transfer in multiple scattering and emitting layered media, Applied Optics, 27, 2502–2509, 1988.

Timco, G. and Frederking, R.: A review of sea ice density, Cold regions science and technology, 24, 1–6, 1996.

Weeks, W.: On sea ice, chap. Snow, pp. 417–433, University of Alaska Press, 2010.